BMC Infectious Diseases

RESEARCH

Open Access

Nucleocapsid protein enhances spike- and RBD-specific humoral and cellular immune responses in protein-based SARS-CoV-2 vaccine

Stina Gröhn[1], Heini Lehto[1], Saana Soppela[1], Rauno A. Naves[2,3], Mikael A. Ritvos[3,4], Alina Iakubovskaia[2], Vili Lampinen[1], Iiris Mustonen[1], Sanniina Pakkala[1], Elizaveta Husu[1], Laura Kakkola[5,6], Ilkka Julkunen[5,6,7], Pekka Kolehmainen[5], Arja Pasternack[2,3], Olli Ritvos[2] and Minna M. Hankaniemi[1*]

Abstract

Background Current COVID-19 vaccines are effective at preventing severe disease but provide limited protection against infection and transmission, particularly as new variants emerge. Vaccines capable of inducing both systemic and mucosal immunity and robust T cell responses, may offer broader and more long-lasting protection. This study aimed to evaluate protein-based vaccine candidates incorporating SARS-CoV-2 spike (S) and its receptor-binding domain (RBD), as well as nucleocapsid protein (N) antigens administered through different immunization schemes.

Methods Mice were immunized three times at four-week intervals with vaccine formulations containing Fc-fused RBD proteins, S, and/or N proteins. Vaccines were administered intranasally, subcutaneously, or with subcutaneous or intramuscular priming followed by intranasal boosting. Branched polyethylenimine (BPEI) was used as a mucosal adjuvant, and Adjuvant system 04 (AS04) for intramuscular administration. Depending on the experiment, BPEI or AS04 was used for subcutaneous immunizations. Systemic antibody responses were assessed from serum samples and mucosal antibody responses from bronchoalveolar lavage samples by ELISA. Cellular responses were measured from splenocytes after antigen stimulation by FluoroSpot analysis of cytokine secretion.

Results Fc-fused RBD antigens elicited higher antibody responses than whole S protein. Inclusion of low amount of N protein enhanced RBD- and S-specific systemic and mucosal IgG and IgA responses, and significantly increased splenocyte IL-2 and IFN-γ secretion. Intranasal vaccination alone induced variable mucosal antibody responses, whereas intramuscular priming followed by intranasal boosting consistently produced higher systemic IgG levels, robust mucosal responses, and T cell activity. Neutralizing antibodies were negligible in intranasally primed groups but were detectable in most animals receiving intramuscular priming. Among all regimens, the combination of intramuscular priming with N-containing formulations generated the highest magnitude and breadth of humoral and cellular responses. All vaccine formulations were well tolerated with no adverse effects observed.

*Correspondence:
Minna M. Hankaniemi
minna.hankaniemi@tuni.fi

Full list of author information is available at the end of the article

Conclusions Protein-based vaccines incorporating N together with Fc-fused RBD antigens significantly broaden and enhance immune responses in mice. Intramuscular priming followed by intranasal boosting proved superior to other regimens, inducing strong systemic, mucosal, and cellular immunity. These findings suggest that inclusion of conserved internal virus antigens and heterologous prime-boost strategies may improve durability and breadth of protection, supporting their development as next-generation COVID-19 vaccines.

Keywords SARS-CoV-2 virus, Next-generation COVID-19 vaccines, Coronaviruses, Protein subunit vaccines, Intranasal vaccination, Immunogenicity, Nucleocapsid protein, Fc-fused RBD protein

Graphical Abstract

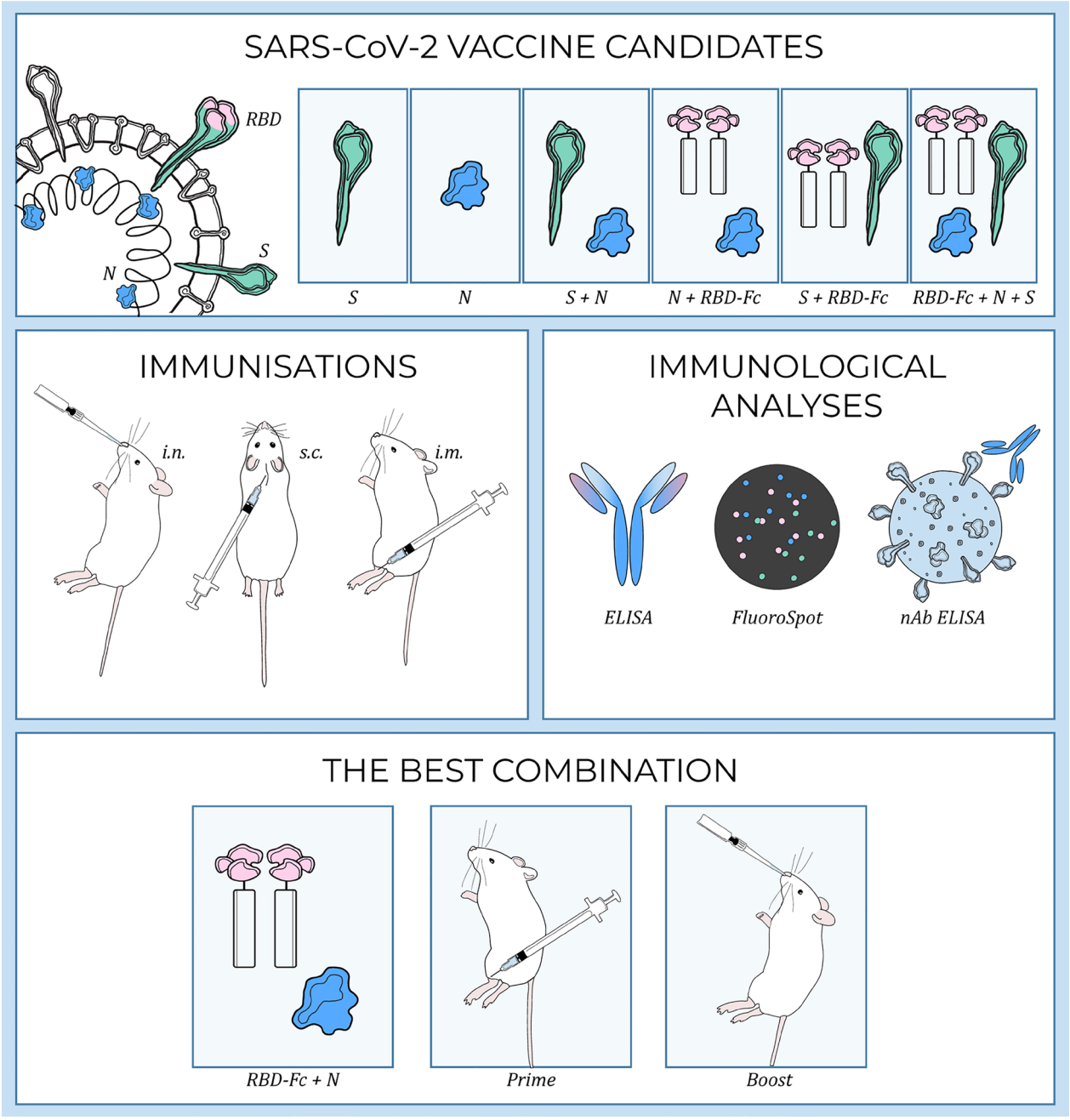

Background

Coronaviruses (CoVs) are a diverse group of enveloped positive-sense single-stranded RNA viruses belonging to the subfamily Orthocoronavirinae, in the family *Coronaviridae* of the order *Nidovirales*. There are four endemic, human CoVs (HCoVs) circulating in the human population: HCoV-229E, HCoV-NL63, HCoV-HKU1 and HCoV-OC43, which are generally associated with relatively mild clinical symptoms and typically cause common colds. The first highly pathogenic HCoV emerged in 2002 in China [1]. It caused a deadly outbreak with a mortality rate of approximately 10% during 2002–2004 before it disappeared [2]. This novel CoV was designated Severe Acute Respiratory Syndrome Coronavirus (SARS-CoV), named after the new human illness it caused. A second novel CoV, Middle East Respiratory Syndrome Coronavirus (MERS-CoV), appeared in Saudi-Arabia in 2012. The virus was responsible for outbreaks in South Korea in 2015 and in Saudi Arabia in 2018, and it continues to circulate among the camels mainly in the Arabic peninsula [1]. In late 2019, another novel CoV emerged in Wuhan, China [3]. The World Health Organization (WHO) named this virus Severe Acute Respiratory Syndrome Coronavirus 2 (SARS-CoV-2) and the disease Coronavirus disease 2019 (COVID-19). To date (27 October 2025), the COVID-19 pandemic has caused over 778 million cases and over 7.1 million deaths [4].

The genome of SARS-CoV-2 encodes 16 non-structural proteins and four major structural proteins: spike (S), envelope (E), membrane (M), and nucleocapsid (N) proteins. S, E, and M proteins form the capsid of SARS-CoV-2, while the N protein resides inside the capsid to pack the genomic RNA. S protein is particularly important for the virus, as it contains a vital receptor-binding domain (RBD), which is responsible for the recognition of host cell surface receptors that enable virus entry [5]. Since S protein protrudes prominently from the viral surface, it is also a direct target for host immune responses, making it the major target of neutralizing antibodies [6].

Prior to SARS-CoV, MERS-CoV and SARS-CoV-2 outbreaks, coronavirus vaccine development was focused solely on veterinary CoVs and routinely used to prevent serious disease in young animals [1]. SARS-CoV and MERS-CoV outbreaks sped up the vaccine development for CoVs. Various forms of vaccines targeting SARS-CoV and MERS-CoV were developed and tested in preclinical models. However, only a few of them entered clinical trials and none of them were approved by the U.S. Food & Drug Administration (FDA) [7–9]. The subunit vaccines developed against SARS-CoV and MERS-CoV were mainly based on the full-length S protein or on the RBD domain due to their ability to induce neutralizing antibodies against the virus [10]. Additionally, a few N and M protein-based SARS-CoV vaccines were developed and preclinically tested, because several immunodominant B and T cell epitopes have been identified in these proteins [11–13]. With the emergence of SARS-CoV-2, the coronavirus vaccine development scene exploded. In response to the COVID-19 pandemic, extensive efforts were undertaken globally to develop effective vaccines. Many of these received emergency authorisation from both the European Medicines Agency (EMA) and FDA. While these vaccines have reduced the global burden of COVID-19 disease, they remain insufficient in the combat against SARS-CoV-2. In 2023, there were over 380 vaccines in different stages of pre-clinical or clinical trials. Out of the 183 vaccines in different clinical phases, most were utilizing protein subunit (32%) or RNA (24%) platforms and non-mucosal administration routes (89.6%). For the vaccines in pre-clinical phase, protein subunit (38.7%) and viral vectors (22.1%) were the most utilized platforms [14]. Currently, there are only five EMA authorised COVID-19 vaccines on the market: Bimervax (previously COVID-19 Vaccine HIPRA) by HIPRA Human Health S.L.U., Comirnaty developed by BioNTech and Pfizer, Kostaive by Arcturus Therapeutics Europe B.V., Nuvaxovid by Novavax CZ, a.s., and Spikevax (previously COVID-19 Vaccine Moderna) by Moderna Biotech Spain S.L. [15]. These current vaccines provide 56–95% efficacy against symptomatic COVID-19, but for persistent immunity booster immunizations are required [16–19]. In addition to waning immunity, a key limitation of the current vaccines is their intramuscular administration. While intramuscularly administered COVID-19 vaccines provide robust systemic antibody responses and prevent the incidence of severe disease, they cannot fully prevent infection and transmission leading to breakthrough infections [20–22].

Therefore, inducing a local mucosal immune response could be an effective way to protect against SARS-CoV-2 infection and transmission. In order to establish respiratory immunity with resident memory T and B cells in the upper airways and lungs, the vaccine must be administered locally in the respiratory tract [23, 24]. Intramuscular administration of SARS-CoV-2 vaccines induces high levels of circulating antibodies, memory B cells, and circulating effector CD4+ and CD8+ T cells in animal models and humans [25–27]. However, non-mucosal vaccines do not induce high levels of potent antiviral immune memory at mucosal surfaces, such as tissue-resident memory B cells (BRM cells) and T cells (TRM cells) as well as mucosal immunoglobulin G (IgG) and dimeric IgA [28–31]. Vaccines targeting the respiratory mucosa could address the shortcomings of non-mucosal vaccination; recent assessments of intranasally delivered

SARS-CoV-2 spike encoding adenoviral vectors and recombinant spike proteins have shown mucosal immunogenicity as well as protection and reduced viral shedding in mice, hamsters, and nonhuman primates [31–39].

Key factors for a mucosally administered protein-based vaccine against COVID-19 include effective antigen presentation, robust immune activation, and long-lasting protection [40, 41]. Engineering of the Fc (fragment, crystallizable) portion of an immunoglobulin (Ig) offers a promising way to achieve these goals by optimizing interactions with immune cells. Incorporating the Fc portion of an IgG molecule into a vaccine antigen provides several immunological advantages. The IgG Fc portion enables targeted binding to Fc-gamma receptors (FcγRs) on antigen-presenting cells (APCs), facilitating efficient antigen uptake, processing and presentation to T cells [42–45]. This process is critical for initiating a strong adaptive immune response. Inducing antigen specific T cell responses via MHC:antigen peptide-T cell receptor (TCR) is essential for mounting long-lasting, effective immunity which in the case of soluble protein antigens is to a considerable extent controlled by FcγR function [45]. Furthermore, Fc-mediated effector functions, such as antibody-dependent cellular cytotoxicity (ADCC) and antibody-dependent cellular phagocytosis (ADCP), amplify the antiviral activity of the vaccine-induced antibodies [44, 45]. The Fc portion of IgG also interacts with the neonatal Fc receptor (FcRn), which mediates the transfer of IgG across epithelial cells [46, 47]. Within epithelial cells in the endosome or on the cell surface, the FcRn-IgG goes through a non-degradative vesicular transport pathway and the FcRn transports its bound IgG or, in the case of vaccine, the Fc fused antigen across the mucosal barrier and releases it into the lumen or submucosa upon exposure to physiological pH [48]. Through binding, FcRn also extends the half-life of IgG and, therefore, the half-life of Fc fused antigen [49]. This prolonged exposure enhances both the magnitude and durability of the immune response, making Fc-fusion strategies a compelling approach for next-generation COVID-19 vaccines.

In addition to enhancing the immune response with Fc engineering, the role of mucosal adjuvants is critical in developing mucosally administered protein-based vaccines [50]. Protein-based vaccines usually lack endogenous innate immune stimulators possessed by live attenuated or killed whole pathogens, such as bacterial cell wall products and genomic nucleic acids, which act as pathogen-associated molecular patterns (PAMPs) and are able to induce adaptive immune responses [51]. Although adjuvant requirements are mostly the same for parenteral and mucosal vaccines, the development of mucosal vaccine adjuvants requires specialized considerations of adapting the adjuvants to characteristic mucosal conditions. Currently, there are no mucosal adjuvants that hold market approval or are in clinical use. The most studied and potent mucosal adjuvants are cholera toxin (CT), the heat-labile toxin (LT) produced by *Escherichia coli* and diphtheria toxin. These toxins have an adjuvant effect and are considered to be a gold standard of mucosal adjuvants. However, due to their harmful toxic effect, they are not used for clinical application [52]. Although to avoid these toxic effects, mutants that are less toxic have been created [53, 54]. Molina Estupiñan and colleagues have recently used dmLT (double mutant detoxified version of the heat-labile enterotoxin) and mmCT (non-toxic multiple mutant of cholera toxin) in their study to adjuvant intranasally administered pneumococcal conjugate vaccine [55]. Another class of adjuvants is the pattern recognition receptors (PRRs) ligands. These adjuvants are based on PAMPs activation and act through Toll-like receptor (TLR) stimulus. Examples of these kinds of adjuvants, which have been administered intranasally in preclinical phases, are CpG oligodeoxynucleotides (ODNs) [31] and polyinosinic-polycytidylic acid (Poly(I:C)) [56]. In addition, cytokines and chemokines have been shown to work in mucosal sites as adjuvants [52]. An adjuvant (CP-15) combining two TLR agonists, CpG ODNs and poly(I:C), with cytokine IL15, has been used as a mucosal adjuvant in a preclinical SARS-CoV-2 study [39]. Adjuvants can also be classified as delivery adjuvants which comprise nano- or microparticles, polymers, emulsion, liposomes and immune-stimulating complexes (ISCOM) that are used to encapsulate the antigen and deliver it to a specific cell [52]. Intranasally administered examples of these in preclinical studies are Montanide ISA™ 51 (blend of mannide monooleate surfactant and mineral oil) [57], Alhydrogel® [58] and polyethyleneimine (PEI) [53, 54]. An oil-in-water adjuvant, $W_{80}5EC$ (NanoVax®), has even been tested in clinical phase [59].

In this study, we developed and evaluated a protein-based SARS-CoV-2 vaccine strategy guided by two related hypotheses. First, we hypothesized that the inclusion of the conserved SARS-CoV-2 nucleocapsid protein in spike-containing formulations would broaden the cellular immunity, particularly T cell responses. Second, we hypothesized that mucosal delivery of S- and N-containing protein vaccines, in combination with selected adjuvants, would elicit an immune profile distinct from conventional parenteral vaccination, characterized by enhanced mucosal and cellular immunity. To test these hypotheses, we systematically optimized antigen composition, dosage,

and route of administration using whole N and S proteins as well as Fc-fused RBD domains from multiple SARS-CoV-2 variants (Wuhan, beta B.1.351, and omicron BA.4/BA.5) at different doses in a murine model. We compared intranasal, subcutaneous, and intramuscular immunization strategies and additionally assessed branched PEI (BPEI) as a potential mucosal adjuvant. Our findings demonstrate that incorporating a low amount of N protein into RBD-based formulations and using an intramuscular prime – intranasal boost strategy substantially enhances the breadth and durability of both humoral and cellular immunity. Importantly, identifying an optimal antigen combination and administration strategy provides a framework for rational design of next-generation COVID-19 vaccines capable of eliciting more cross-protective and long-lasting immunity. Further work is needed to define the most effective mucosal adjuvant to support this approach.

Methods

Design of the vaccine antigens

The N protein was produced based on the original SARS-CoV-2 strain (first identified in Wuhan, GenBank ID: YP_009724397.2). Prefusion stabilized S protein was produced based on SARS-CoV-2 Alpha strain (B.1.1.7, GenBank ID: QQX99439.1). The design of the spike protein is similar as the design described previously [60]. Six amino acids (K986, V987, F817, A892, A899, and A942) in the S2 portion of the S head region were replaced with 6 prolines. The furin cleavage site was mutated from RRAR to AGAG (residues 682–685) to prevent S1–S2 cleavage [61], and the C-terminal transmembrane/cytoplasmic tail domain of S was replaced with a T4 fibritin self-trimerizing domain (GenBank ID: 1RFO_A).

The genes for S and N proteins were codon optimized for insect cell expression and synthesized by GenScript Biotech (Piscataway, NJ, USA). The S coding gene was cloned downstream of the polyhedrin promoter and honeybee melittin signal sequence [62] in the pOET5 plasmid vector (Oxford Expression Technologies, Oxford, UK) along with the addition of C-terminal 8xHis tag. The N coding gene was cloned downstream of p10 promoter in the pOET5 plasmid vector (Oxford Expression Technologies) without the inclusion of an affinity purification tag.

SARS-CoV-2 S-protein RBD domain variants were designed to be produced in mammalian cells based on strains of the original (Wuhan, GenBank ID: NC_045512.1), the beta (B.1.351, first identified in South Africa, GenBank ID: OR939248) and subvariants of omicron (omicron BA.4/BA.5, GenBank IDs: OP093374 and OP093373, respectively). A codon optimized synthetic 1531 bp cDNA (GenBank ID: PP599180.1) encoding SARS-CoV-2 RBD amino acids 319–541 as an N-terminal fusion protein attached through a 6 amino acid GSGGGG linker to mouse IgG2a Fc part (amino acid residues 238–469) followed by a 10 amino acid GSHHHHHHHH tag was designed based on the original isolate Wuhan-Hu-1 and synthesized by GeneUniversal (Newark, DE, USA). The same construct was used to generate wuRBD-GS-8his by deleting the mFc portion flanked by introduced BamHI restriction enzyme sites. Separate saRBD-GS-8his and BA.4/5-RBD-GS-8his synthetic constructs were generated to cover the respective SARS-CoV-2 RBD 319–541 amino acids of the beta "South Africa" variant and the omicron BA.4/5 variant and these were used for expressing antigens for ELISA. Furthermore, mFc-6his tagged versions of these variants were developed for obtaining saRBD-mFc-6his and BA.4/5-mFc-6his antigens for vaccine formulations. All these RBD cDNA variants were subcloned into a mammalian expression plasmid vector with a CAG-promoter and internal ribosomal entry site driven puromycin selection gene.

Production and purification of vaccine antigens

The N and S proteins were produced and purified similarly as described before for CVB1-VLPs produced in our research group [63]. Briefly, the recombinant baculovirus stocks were generated using flashBAC ULTRA baculovirus kit (Oxford Expression Technologies) according to manufacturer's instructions. The titres of the baculovirus stocks were determined using a BacPAK™ Baculovirus Rapid Titre Kit (TaKaRa, Mountain View, USA).

The N protein was produced in High Five cells in Insect-XPRESS™ Protein-free Insect Cell Medium (Lonza, Basel, Switzerland) using a multiplicity of infection (MOI) value of 1 pfu/cell and cultivation time of 4 days. The cultured supernatant was harvested by filtering the culture with Sartoclear Dynamics® Lab V 1000 mL Kit 0.22 µm pore size (Sartorius, Göttingen, Germany). The N protein was concentrated from the culture supernatant by Tangential Flow Filtration (TFF), utilising 10 MWCO hollow fiber with an ÄKTA Flux system (Cytiva, Marlborough, MA, USA). The buffer was exchanged to 50 mM $NaHPO_4$ (pH 7.4) with the same system. The protein was bound to 5 ml SP FF cation exchange column (Cytiva) in 50 mM $NaHPO_4$ (pH 7.4) buffer and eluted using stepwise NaCl gradient (>95% pure protein peak with 0.5 M NaCl).

The S protein was produced in High Five cells in Insect-XPRESS™ Protein-free Insect Cell Medium (Lonza) using a MOI value of 10 pfu/cell and cultivation time of 5 days or a MOI value of 20 pfu/cell and cultivation time of 4 days. The protein was collected from the culture supernatant by filtering the culture with Sartoclear Dynamics® Lab V 1000 mL Kit 0.22 µm pore size (Sartorius). Prior to chromatography, the supernatant was diluted 1:1 with 50 mM $NaHPO_4$ (pH 7.4) buffer. The protein was bound to HisTrap Excel column (Cytiva) at 4 °C, eluted with stepwise imidazole gradient (>95% pure protein

peak with 0.25 M imidazole), and dialyzed by gradually decreasing imidazole concentration against phosphate buffered saline (PBS) until the imidazole was completely removed from the sample.

SARS-CoV-2 RBD domains fused to mouse IgG2a Fc regions (RBDmFc proteins) were produced in mammalian cells and purified as described before [64]. Briefly, the expression plasmids were transfected to human embryonic kidney (HEK293F) cells with Fugene 6 (Promega, Madison, WI, USA) and selected for stable cell production with puromycin (Gibco, Waltham, MA, USA). The cell line was adapted to suspension culture in CD OptiCHO medium (Gibco) supplemented with 2 mmol/l Ultraglutamine (Lonza) for large-scale production. The cell culture was maintained in a square-bottom glass flask at 37 °C, then shifted to 33 °C for 5–8 days to promote protein production. The culture media were collected and filtered through a 0.22-µm Steritop™ membrane (Merck, Darmstadt, Germany). Recombinant proteins were subsequently captured using either Protino Ni-NTA column (Macherey-Nagel, Düren, Germany) or HisTrap Excel column (Cytiva) at 4 °C, eluted with a gradient of increasing imidazole concentrations, and finally dialyzed against PBS.

Vaccine antigen characterization

Purified vaccine antigens were analysed with Criterion TGX stain-free precast gels (Bio-Rad Laboratories, Hercules, CA, USA). The amount of impurities in the vaccine antigens were assessed by densitometry analysis of stain-free stained SDS-PAGE gels using the ImageJ Fiji software v2.16.0 [65] (https://imagej.net/). Protein concentration was determined with UV/Vis spectroscopy using Nanodrop (Thermo Fisher Scientific, Waltham, MA, USA).

Table 1 Vaccination groups and regimens in the first study

Group	*n*	Vaccine	Dose	Administration route
GR1	6	Buffer	-	2 × s.c.
GR2	6	N	4 µg	2 × s.c.
GR3	6	N	8 µg	2 × s.c.
GR4	6	S	4 µg	2 × s.c.
GR5	6	S	8 µg	2 × s.c.
GR6	6	N + S	4 + 4 µg	2 × s.c.
GR7	6	N + S	8 + 8 µg	2 × s.c.
GR8	3	Buffer	-	2 × i.n.
GR9	3	N + S	2 + 2 µg	2 × i.n.
GR10	3	N + wuRBDmFc	4 +4 µg	2 × i.n.
GR11	3	N + wuRBDmFc	8 + 8 µg	2 × i.n.

A total of 54 female BALB/c mice were randomly assigned to eleven different vaccination groups ($n = 3$ or $n = 6$). Six groups (GR2-7) received two doses of different formulations of the vaccine subcutaneously (s.c.) with a four-week interval and three groups (GR9-11) received two doses of different formulations of the vaccine intranasally (i.n.). GR1 and GR8 were control groups and received PBS instead of the vaccine formulations. wuRBDmFc stands for RBD from the original "Wuhan" strain fused with mouse IgG2a Fc region

The morphologies of N and S proteins as well as the RBDmFc proteins were analysed with mass photometry. Prior to analysis, all the proteins were diluted to a concentration of 200 nM with sterile filtered PBS (Gibco). Before measuring the samples, standard samples with known morphologies and masses were analysed to acquire a standard curve to which sample measurements could be compared to. In this case, the used standards were beta-amylase (Sigma-Aldrich, St. Louis, MO, USA) and thyroglobulin (Sigma-Aldrich). Every measurement was executed in a droplet of filtered PBS so that the measuring concentration of the samples was 20 nM, 40 nM or 100 nM and recorded for 60 seconds. Refeyn TwoMP mass photometer (Refeyn Ltd, Oxford, UK) and AcquireMP software (Refeyn Ltd) were used for the measurements and DiscoverMP software (Refeyn Ltd) for the analysis.

Additionally, endotoxin concentrations were determined from the vaccine antigen stocks with ENDOZYME® II GO STRIPS (BioMerieux, Marcy-l'Étoile, France) and measured with Spark® multimode plate reader (Tecan, Männedorf, Switzerland). The amount of residual DNA in the stocks was measured with Qubit™ 1X dsDNA HS Assay Kit (Invitrogen, Waltham, MA, USA) and Qubit™ fluorometer (Invitrogen).

Vaccine formulation, immunizations, and sampling of mice

All mouse immunizations and sample collections were carried out following similar procedures as previously detailed in our research group's studies on the immunogenicity of the CVB1-VLP and SARS-CoV-2 vaccines [63, 66, 67]. For the first immunization study, vaccines were formulated by diluting the antigens using PBS (Gibco) as a diluent to a final volume of 45 µl for intranasal immunizations and to a final volume of 150 µl for subcutaneous immunizations. 5 µg per dose of MPLA-SM Vaccigrade™ (Invivogen, San Diego, CA, USA) and 50 µg per dose of Alhydrogel® adjuvant 2% (Invivogen) were added prior to administration and vaccine-adjuvant mixtures were mixed for 5 minutes at room temperature (RT) to allow the Alhydrogel to effectively adsorb the antigens. 6-week-old female BALB/cJRj mice (Janvier Labs, Le Genest-Saint-Isle, France) were divided into groups of 3 or 6 mice (Table 1). Seven groups were administered the 150 µl dose subcutaneously (s.c.) on weeks 0 and 4. Four groups were administered the 45 µl dose intranasally (i.n.) by gradually pipetting 22.5 µl of adjuvanted vaccine to each nasal opening on weeks 0 and 4. PBS (Gibco) with adjuvant was used as a negative control. Blood samples from tail veins were collected prior to immunizations on weeks 0, 4, 6, and 8 under inhalation anaesthesia by isoflurane (Attane vet, Vet Medic Animal Health, Hattula, Finland). The blood samples were centrifuged 3500 g for 20 minutes at +4 °C and the subsequent serums were stored at

−80 °C until further use in ELISA. Mice were euthanised on week 10 with CO_2 and whole blood was collected to BD Microtainer® blood collection tubes (Becton Dickinson Biosciences, New Jersey, NJ, USA) through heart puncture.

For the second immunization study, vaccines were prepared by diluting the antigens using PBS (Gibco) as a diluent either to a final volume of 26 µl (i.n. administration) or to a final volume of 150 µl (s.c. administration). 10 µg per dose of 25kDa branched polyethylenimine (BPEI) (Sigma-Aldrich) was added prior to administration and left to incubate for 2 hours at RT. 6-week-old female BALB/cJRj mice (Janvier Labs) were divided into groups of 3 or 6 mice (Table 2). All the groups except for group 5 were administered the 26 µl dose i.n. by gradually pipetting 13 µl of adjuvanted vaccine to each nasal opening of the mouse on week 0, 4 and 8. Group 5 received their first vaccine dose of 150 µl through the s.c. route on week 0 and the next two doses i.n. on week 4 and 8. Blood samples from tail veins were collected on week 0, 4, 6, 8, and 10 under inhalation anaesthesia by isoflurane (Attane vet, Vet Medic Animal Health). The blood samples were centrifuged 3500 g for 20 minutes at +4 °C and the serum specimens were stored at −80 °C until further use in ELISA. Mice were euthanised on week 12 and whole blood was collected to BD Microtainer® blood collection tubes (Becton Dickinson Biosciences) from axillary vein under terminal anaesthesia by a lethal dose of ketamine hydrochloride (Ketaminol vet, MSD Animal Health, Rahway, NJ, USA) and medetomidine hydrochloride (Dorbene vet, Vetcare Oy, Helsinki, Finland). Finally, the euthanisation was ensured by cervical dislocation. The whole blood samples were centrifuged 8000 g for 90 seconds at RT and the serum specimens were stored at −80 °C until further use in ELISA. Additionally, bronchoalveolar lavage (BAL) samples were collected by orotracheal intubation of terminally anaesthetized mice by flushing the lungs with 2 ml of PBS (Gibco) supplemented with EDTA-free Pierce™ Protease Inhibitor Mini Tablets (Thermo Fisher Scientific) using an olive tip cannula (Acufirm, Berlin, Germany) [68]. The BAL samples were centrifuged 20,000 g for 5 min at +4 °C before storing the supernatants at −80 °C until further use in ELISA. Finally, the spleens of the immunized mice were also collected and splenocytes were extracted as follows: spleens were smashed through sterile 40 µm cell strainers (Thermo Fisher Scientific) to get single-cell suspensions and washed with washing buffer containing PBS (Gibco) supplemented with 1% FBS (Sigma-Aldrich) and 2 mM EDTA (Sigma-Aldrich). The cells were centrifuged 400 g for 5 min and red blood cells were lysed with 1 ml of ACK buffer (Gibco) for 1 min. The lysed cells were removed by washing the cells with washing buffer and centrifuged. One final washing step was conducted, the suspensions centrifuged, and then the cells were suspended in washing buffer for cell counting. The cell counting was performed with Countess™ Automated Cell Counter (Invitrogen). After counting, the cells were centrifuged, suspended in freezing buffer consisting of 50% RPMI-1640 Medium (Thermo Fisher Scientific), 40% FBS (Sigma-Aldrich) and 10% DMSO (Sigma-Aldrich) and cryopreserved until further use.

Table 2 Vaccination groups and regimens in the second study

Group	*n*	Vaccine	Dose	Administration route
GR1	3	Buffer	-	3 × i.n.
GR2	6	wuRBDmFc + saRBD-mFc + S	1.3 + 1.3 + 1.3 µg	3 × i.n.
GR3	6	wuRBDmFc + saRBD-mFc + S + 0.5 N	1.3 + 1.3 + 1.3 + 0.5 µg	3 × i.n.
GR4	6	wuRBDmFc + saRBD-mFc + S + N	1.3 + 1.3 + 1.3 + 1 µg	3 × i.n.
GR5	6	wuRBDmFc + saRBD-mFc + S + N	1.3 + 1.3 + 1.3 + 1 µg	1 × s.c. + 2 × i.n.

A total of 27 female BALB/C mice were randomly assigned to five different vaccination groups ($n = 3$ or $n = 6$). Three groups (GR2-4) received three doses of different formulations of the vaccine intranasally (i.n.) with four-week intervals. One group (GR5) received the first dose subcutaneously (s.c.) and the following two doses i.n. GR1 was a control group and received PBS instead of the vaccine formulations. wuRBDmFc stands for RBD from the original "Wuhan" strain fused with mouse IgG2a Fc region and saRBDmFc for RBD from the beta "South Africa" strain fused with mouse IgG2a Fc region

For the third immunization study, vaccines were prepared by diluting the antigens using PBS (Gibco) as a diluent either to a final volume of 26 µl (i.n. administration) or to a final volume of 50 µl (intramuscular administration). 10 µg per dose of BPEI (Sigma-Aldrich) was added prior to i.n. administration and left to incubate for 2 hours at RT. Prior to intramuscular (i.m.) administration, 5 µg per dose of MPLA-SM Vaccigrade™ (Invivogen) and 50 µg per dose of Alhydrogel® adjuvant 2% (Invivogen) were added and the vaccine-adjuvant mixtures were mixed for 5 minutes at RT to allow the Alhydrogel to effectively adsorb the antigens. 6-week-old female BALB/cJRj mice (Janvier Labs) were divided into groups of 5 or 8 mice (Table 3). Groups 1–3 were administered the 26 µl dose i.n. by gradually pipetting 13 µl of adjuvanted vaccine to each nasal opening on weeks 0, 4 and 8. Groups 4 and 5 received their first vaccine dose of 50 µl through the i.m. route on week 0 and the next two doses i.n. on weeks 4 and 8. 5 mice of each group were euthanised on week 12 and 3 mice from groups 2 to 5 were followed up for eight weeks and euthanised on week 20. Blood samples were collected from the follow-up mice on weeks 14, 16, and 18. All the sample collection, handling and the following procedures were performed as in the previous animal study (second immunisation study) with the exception that the extracted splenocytes were suspended

Table 3 Vaccination groups and regimens in the third study

Group	*n*	Vaccine	Dose	Administration route
GR1	5	Buffer	-	3 × i.n.
GR2	8	BA.4/5 RBDmFc	4 µg	3 × i.n.
GR3	8	BA.4/5 RBDmFc + N	4 + 0.5 µg	3 × i.n.
GR4	8	BA.4/5 RBDmFc	4 µg	1 ×i.m. + 2 × i.n.
GR5	8	BA.4/5 RBDmFc + N	4 + 0.5 µg	1 × i.m. + 2 × i.n.

A total of 37 female BALB/C mice were randomly assigned to five different vaccination groups ($n=5$ or $n=8$). Groups 2 and 3 received three doses of different formulations of the vaccine intranasally (i.n) with four-week intervals. Groups 4 and 5 received the first dose intramuscularly (i.m.) and the following two doses i.n. GR1 was a control group and received PBS instead of the vaccine formulations. BA.4/5 RBDmFc stands for RBD containing the mutations from both the BA.4 and BA.5 subvariant of omicron strain fused with mouse IgG2a Fc region

in splenocyte incubation medium consisting of RPMI 1640 Medium supplemented with GlutaMAX (Thermo Fisher Scientific), 500 U Penicillin-Streptomycin (Sigma-Aldrich), 10% FBS (Sigma-Aldrich), and 25 mM HEPES (Sigma-Aldrich) for cell counting and used directly for FluoroSpot assays without cryopreserving them first.

Prior to the start of the pre-clinical experiments, all animals were randomly divided into the groups and allowed to acclimate for 7 days. All mice were housed in pathogen-free environment in individually ventilated NexGen™ IVC cages (Allentown LLC, Allentown, NJ, USA) and food and water were provided ad libitum. The pre-clinical experiments were done in accordance with the regulations and guidelines of the Finnish National Experiment Board (Permission number ESAVI/48887/2023). All efforts were made to minimize animal suffering and to reduce the number of animals used. The welfare of the animals was monitored throughout the experiment and Animal Research: Reporting of In Vivo Experiments (ARRIVE) guidelines were followed. The laboratory animal usage permission (Regional State Administrative Agency, Pirkanmaa, Finland; decision number ESAVI/1408/2021) held by the research group (Virology and Vaccine Immunology at the Tampere University) covers all animal experiments conducted in this study.

Antigens for immunological analyses

The N and S protein based on the same antigens as in the vaccinations were used in this study in measuring the antigen-specific immunoglobulin levels in ELISA analyses and as stimulants in FluoroSpot analyses. For measuring the RBD-specific immunoglobulin levels from sera and mucosal samples, RBD proteins without the IgG2a Fc region were produced. Briefly, RBD cDNAs were subcloned with C-terminal 8×His tag into a mammalian expression plasmid vector with a CAG-promoter and internal ribosomal entry site driven puromycin selection gene. Puromycin selection, protein expression, purification and characterization were done with same methods as described earlier for the RBDmFc vaccine antigens in this study.

Antigen specific IgG and IgG subtype antibodies in serum

Antigen specific IgG, IgG_1 and IgG_{2a} antibodies were determined with indirect enzyme-linked immunosorbent assays (ELISA) from serum samples. F96 Maxisorp Nunc-Immuno plates (Thermo Scientific) were coated with 10 mM carbonate buffer (pH 9.4) containing 50 ng of N protein, 100 ng of S protein or 25 ng of RBD domain without the mFc fragment per well and incubated overnight at RT. After washing the plates with washing buffer (PBS supplemented with 0.85% NaCl and 0.05% Tween20) the plates were blocked with PBS buffer containing 0.1% bovine serum albumin (BSA) (Sigma-Aldrich). EIA buffer (PBS supplemented with 2% NaCl, 1% BSA and 0.05% Tween20) was used as a dilution buffer. Serially diluted mouse sera from the immunization experiment were added to the wells after blocking and incubated for an hour at 37 °C. After incubation, the plates were washed and horseradish peroxidase (HRP) conjugated anti-mouse secondary antibodies IgG (diluted 1:2300 in EIA, Vector Laboratories, Newark, CA, USA), IgG_1 (diluted 1:2300 in EIA, Invitrogen) or IgG_{2a} (diluted 1:2300 in EIA, Invitrogen) were added to the wells and incubated for an hour at 37 °C. After washing, the antigen specific IgG and IgG subtype antibodies were detected using o-Phenylenediamine (OPD) substrate (Sigma-Aldrich). Measurement of absorbance was performed at 490 nm with VICTOR® Nivo™ microplate reader (Revvity, Waltham, MA, USA).

Positivity cut-off value for the end-point titre was determined as previously described in [63]. Briefly, the positivity cut-off value for the end-point titre was established using buffer (PBS) mouse OD readings and calculated as the mean OD plus three times the standard deviation. The end-point titre for each antibody was defined as the highest dilution exceeding this calculated cut-off. Individual sample titres were then plotted, and the results were presented as the geometric mean titre (GMT) for each experimental group. For consistency, the positivity cut-off was assigned an arbitrary value equivalent to one fourth of the starting titre for the 2-fold serum dilutions, corresponding to a 1:100 dilution for serum.

Antigen specific IgA and IgG antibodies in bronchoalveolar lavages

Antigen specific IgA and IgG antibodies were determined from BAL samples with indirect ELISA similarly to the IgG antibodies from serum. The only exception was the secondary antibody used in IgA ELISA assays. In this case, HRP-conjugated goat anti-mouse IgA secondary antibody (1:1000 diluted in EIA, Invitrogen) was used to detect IgA antibodies. Positivity cut-off value

was determined exactly as with IgG antibodies. Endpoint titre values for each sample were plotted in graphs expressing the GMT of each experimental group. The positivity cutoff value was given an arbitrary value of one fourth of the titre of which the 2-fold BAL dilutions were started (positivity cutoff being 1:2.5 dilution for BAL samples).

Neutralizing antibodies in termination serum

The neutralization ability of the antibodies was determined from termination serum samples with SARS-CoV-2 Neutralizing Antibody ELISA Kit (Omicron BA.4/BA.5/BF.7/BQ.1/XBB.1.5) (GeneTex, Irvine, CA, USA). The assay was set up in duplicate and performed according to the manufacturer's instructions. Briefly, the needed number of 8-well strips pre-coated with recombinant ACE2 protein were placed in a holder. Positive control (PC) and negative control (NC) provided in the kit and undiluted termination serum samples were added to the wells together with a working solution of His-tagged BA0.4/5 RBD protein provided in the kit. This mixture was incubated at RT for 1.5 h and then the strips were washed with wash buffer provided in the kit. A working conjugate solution containing HRP-conjugated Anti-His Tag antibody was added to the wells and incubated at RT for 1 h. The strips were then washed and TMB solution was added to each well. The strips were incubated in the dark for 15 minutes and the reaction was stopped with Stop solution provided in the kit. Measurement of absorbance was performed at 450 nm with VICTOR® Nivo™ microplate reader (Revvity). The inhibition rate was calculated using the following formula: Inhibition rate (IR) = [1-(average absorbance value of tested serum sample/average absorbance value of NC)]*100%. Neutralization effect was determined to be present if the IR value was over 30%.

T-cell specific cytokine secretion from stimulated splenocytes

Prior to starting the FluoroSpot assays, cryopreserved splenocytes from vaccinated mice were thawed in splenocyte incubation medium consisting of RPMI 1640 Medium supplemented with GlutaMAX (Thermo Fisher Scientific), 500 U Penicillin-Streptomycin (Sigma-Aldrich), 10% FBS (Sigma-Aldrich), and 25 mM HEPES (Sigma-Aldrich) and rested for 1 h at 37 °C in a humified incubator with 5% CO_2.

Simultaneous secretion of IFN-γ, IL-2, and TNF was analysed with Mouse IFN-γ/IL-2/TNF-α FluoroSpot-PLUS kit (Mabtech, Stockholm, Sweden) as previously described [63, 69]. The assay was set up in duplicate under sterile conditions and the splenocytes of individual mice were tested separately according to the manufacturer's instructions. Briefly, the plates pre-coated with monoclonal antibodies (mAbs) AN18, 1A12, and MT1C8/23C9 from the kit were washed with sterile PBS (Gibco) and blocked with splenocyte incubation medium. After blocking, 1 µg of stimulant (antigen) diluted in splenocyte incubation medium together with 250,000 splenocytes were added to each well and incubated at 37 °C in a humified incubator with 5% CO_2 overnight. Concanavalin A (Sigma-Aldrich) (2 µg/well) and splenocyte incubation medium were used as positive and negative controls, respectively. Additionally, anti-CD28 mAb (diluted 1:1000 in splenocyte incubation medium) from the kit was used as a co-stimulator in each well to enhance antigen-specific responses, as recommended by the manufacturer. After the overnight incubation, the cells were removed by washing the plates with sterile PBS. The detection antibodies were diluted in PBS containing 0.1% BSA (1:200 BAM-tagged anti-IFN-γ mAb, 1:500 biotinylated anti-IL-2 mAb and 1:200 WASP-tagged anti-TNF-α mAb) and added to the plates. The plates were then incubated for 2 hours at RT and washed with sterile PBS. Subsequently, anti-BAM-490, Streptavidin-550, and anti-WASP-640 fluorophore conjugates (diluted 1:200 in PBS+0.1% BSA) were added to the plates, which were incubated for 1 hour at RT. The plates were then washed with sterile PBS and Fluorescence enhancer provided in the kit was added. After a 15-minute incubation at RT, the Fluorescence enhancer and the underdrains from the plates were removed. Plates were then dried and shipped to Mabtech for automated spot analysis with Mabtech IRIS 2 FluoroSpot reader and the numbers of cytokine-secreting cells specifically activated by a stimulant were received as a readout. For each mouse and stimulant used, an average of the duplicate wells was calculated, and the positivity cut-off value subtracted. The positivity cut-off value was determined for each mouse separately as the average number of spots in the negative control wells + 3*(standard deviation). The final frequencies of responding cells were expressed as the number of spot-forming units/10^6 splenocytes.

Statistical analysis

Statistical analyses were done with GraphPad Prism 10.0.1. Immunological data was treated as non-parametric and the comparison between groups was done using Kruskal Wallis test followed with Dunn's Multiple Comparison test.

Results

Production, purification and characterization of the vaccine antigens

In the present study, we produced recombinant vaccine antigens based on N protein, secreted S protein and secreted RBD domains. The N protein did not contain any amino acid modifications, whereas the S protein was

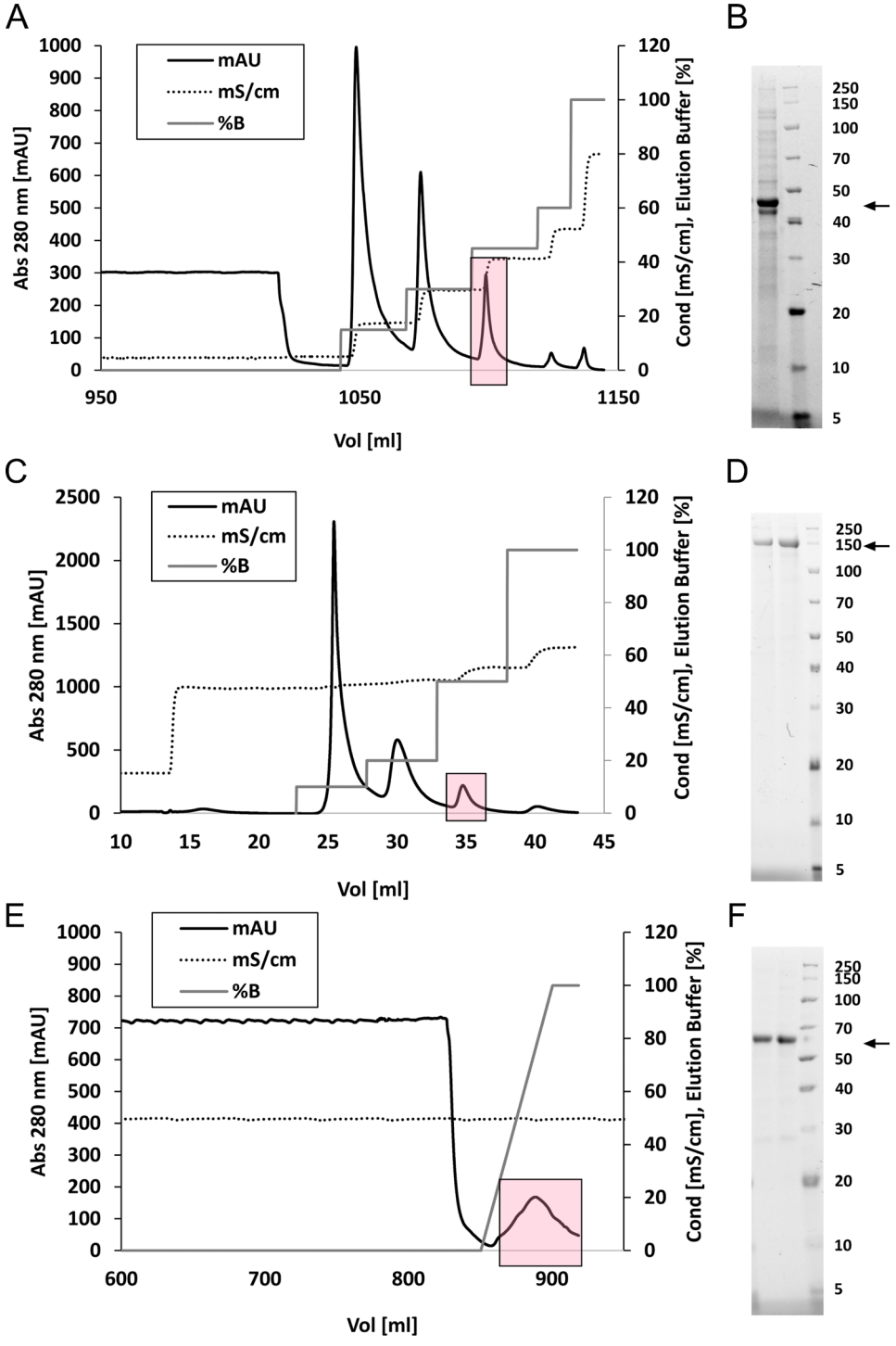

Fig. 1 (See legend on next page.)

stabilized by two mutations in the furin cleavage site to prevent the S1/S2 cleavage as well as 6 strategic amino acids replaced with prolines in the S2 region as previously has been done for the original SARS-CoV-2 spike-protein [60, 70]. For the prefusion state stabilized spike, a T4 fibritin trimerization domain was also included to make the vaccine antigen closely resembling the native spike-protein conformation.

The N protein was purified using cation exchange chromatography. The N protein was captured to SP FF cation exchange chromatography column and eluted from the column using stepwise NaCl gradient. The pure N protein eluted from the column with 0.5 M NaCl (boxed red

(See figure on previous page.)

Fig. 1 Chromatography purification and characterization of the purified vaccine antigens. (**A**) In the chromatography purification step of nucleocapsid protein (N), a buffer containing 50 mM NaHPO4 (pH 7.4), was used as the running buffer, and the same buffer containing 1 M NaCl was used as the elution buffer. After sample loading, unbound proteins were washed out from the column with running buffer and column-bound N proteins eluted at approximately 0.5 M NaCl. Boxed red area indicates the peak belonging to N protein. (**B**) SDS-PAGE analysis and stain-free total protein staining of the purified N protein (N protein indicated by arrow). Full gel image can be found in Additional file 1: Supplementary Fig. 1A. (**C**) In the chromatography purification step of prefusion stabilized spike (S) protein, a buffer containing 50 mM NaHPO4 (pH 7.4), was used as the running buffer, and the same buffer containing 0.5 M imidazole was used as the elution buffer. After sample loading, unbound proteins were washed out from the column with running buffer and column-bound S proteins eluted at approximately 0.25 M imidazole. Boxed red area indicates the peak belonging to S protein. (**D**) SDS-PAGE analysis and stain-free total protein staining of the purified S protein (S protein indicated by arrow). Full gel image can be found in Additional file 1: Supplementary Fig. 1B. (**E**) Representative image of RBDmFc purification process. In the chromatography purification step of RBDmFc proteins, a buffer containing 50 mM NaHPO4 (pH 7.4) and 5 mM imidazole was used as the running buffer, and the same buffer containing 0.5 M imidazole was used as the elution buffer. After sample loading, unbound proteins were washed out from the column with running buffer and column-bound RBDmFc proteins eluted at approximately 0.25 M imidazole. Boxed red area indicates the peak belonging to RBDmFc protein. Here the purified protein is BA.4/5 RBDmFc. (**F**) SDS-PAGE analysis and stain-free total protein staining of the purified RBDmFc protein (RBDmFc protein indicated by arrow). Full gel image can be found in Additional file 1: Supplementary Fig. 1C

area in Fig. 1A). SDS-PAGE analysis and the subsequent detection of the purified proteins with a stain-free staining method (Fig. 1B) revealed proteins of approximately 46 kDa corresponding to the SARS-CoV-2 N protein. The final yield of the ≥95% pure N-protein was 90 mg/l.

The S protein was purified with immobilized nickel-affinity chromatography. The protein was eluted from the column with stepwise imidazole gradient with 0.25 M imidazole (boxed red area in Fig. 1C). SDS-PAGE analysis and the subsequent detection of the purified proteins with a stain-free staining method (Fig. 1D) revealed proteins of approximately 140 kDa corresponding to the SARS-CoV-2 S protein. The final yield of the ≥95% pure S protein was moderate (2.3 mg/l).

SARS-CoV-2 RBDmFc proteins were also purified with immobilized nickel-affinity chromatography. RBDmFc protein was eluted with increasing imidazole concentration and pure protein eluted with approximately 0.25 M imidazole (boxed red area in Fig. 1E). SDS-PAGE analysis and the subsequent detection of the purified proteins with a stain-free staining method (Fig. 1F) revealed proteins of approximately 55 kDa corresponding to the SARS-CoV-2 RBDmFc protein. The final yields of the ≥95% pure RBDmFc proteins were 1000 mg/l (original "Wuhan" strain), 1300 mg/l (Beta, "South Africa" strain) and 800 mg/l (omicron BA.4/5).

To assess the oligomerization status of the vaccine antigens, we used mass photometry. Mass photometry measures light scattering of single particles as they adsorb onto a glass microscope slide allowing rapid determination of mass and oligomeric state of different macromolecules. Based on the results received from the mass photometry measurements, the N protein is a monomer with a mass of approximately 42 kDa as expected (Fig. 2A). In contrast, the S protein, produced in insect cell, was mostly in monomeric form (~124 kDa), with a subset forming possibly tetramers (~564 kDa) (Fig. 2B). With the RBD domains, we utilized Fc engineering in the vaccine antigen design and hypothesized that fusing a mouse Fc fragment to an RBD domain would dimerize the RBD domain and, thus, make it better recognizable by antigen presenting cells and, therefore, more immunogenic. The monomer mass calculated from the sequences is 55 kDa for every RBDmFc protein. According to the measurements, the C-terminally fused RBDmFc proteins seem to dimerize (size range of approx. 120 to 125 kDa) and even oligomerize into bigger structures (tetramers 244–249 kDa, hexamers 363–370 kDa, and octamers 493–495 kDa) through the disulfide bridge present in the Fc region (Fig. 2C, E and G). Fc region may also provide the protein enhanced stability, but also immunogenicity as non-linear epitopes may be conformational epitopes in the dimerized protein. To confirm this Fc dimerization/oligomerization, we also analysed the RBD domains without the Fc fragment fusion. As expected, these RBD domains are in monomeric form and in the size range of approximately 35 to 40 kDa (Fig. 2D, F and H) which is in accordance with the masses calculated from the sequences (approx. 28 kDa) with the approximated mass of glycosylation added.

Additionally, all recombinant proteins used in vaccinations were confirmed to contain < 7.8 ng dsDNA per dose and <1.5 EU endotoxins per µg of vaccine antigen, meeting the criteria set for preclinical experimental vaccines [71, 72].

Recombinant protein-based vaccine induces antigen-specific IgG in serum after subcutaneous and intranasal immunization in mice

After producing, purifying and characterizing the vaccine antigens, we conducted a preclinical pilot study aiming to assess the immunogenicity of the vaccine antigens and determining the optimal dosing regimen for the vaccine candidates. Additionally, we tested the intranasal administration route. We used adjuvant system 04 (AS04) as an adjuvant in the pilot study. AS04 consists of aluminium hydroxide and monophosphoryl lipid A (MPLA) and is a well-established, clinically used parenteral adjuvant [73]. Mice were vaccinated two times with a four-week interval either via subcutaneous (Fig. 3A) or intranasal (see

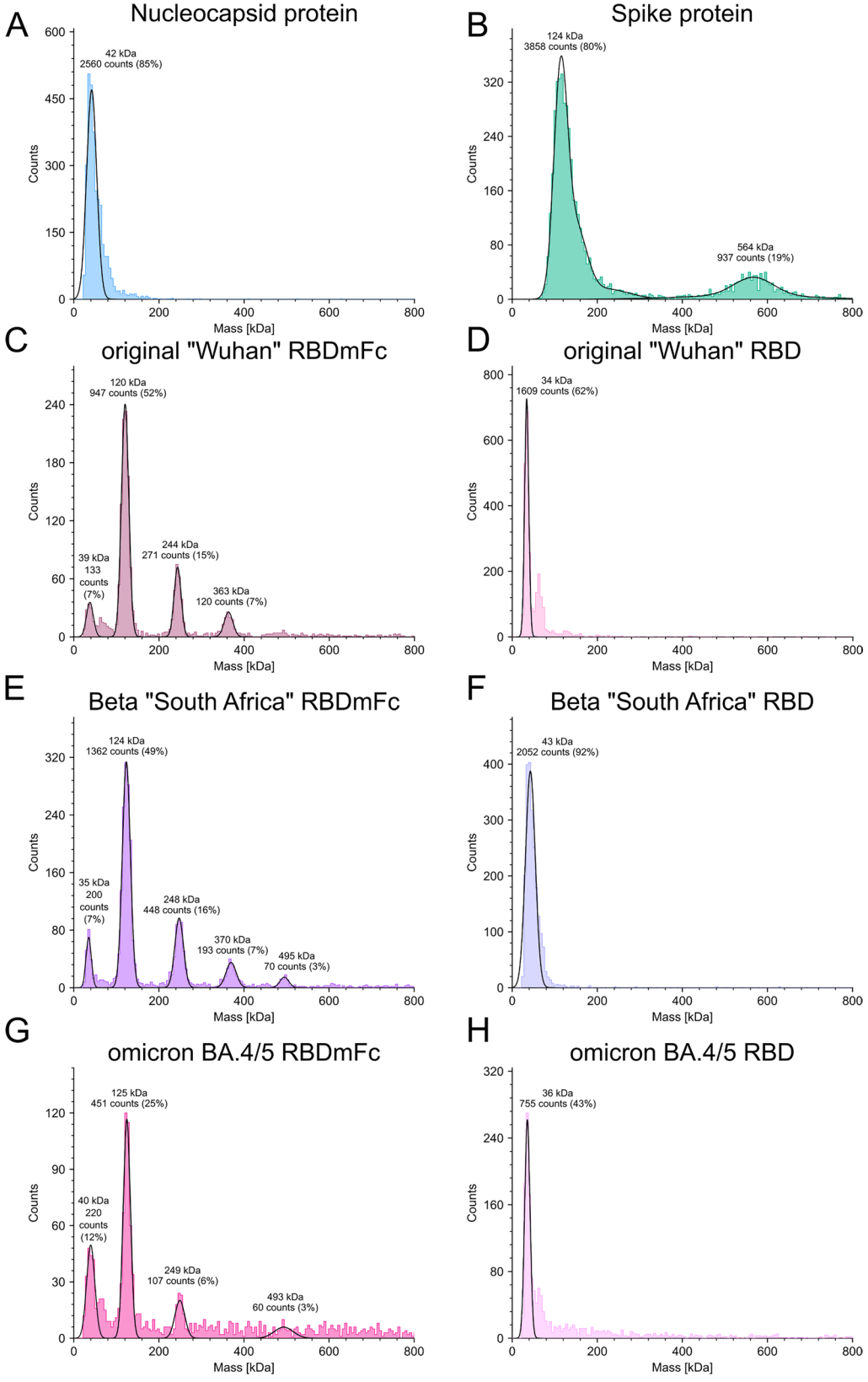

Fig. 2 (See legend on next page.)

(See figure on previous page.)

Fig. 2 Morphology analysis of the vaccine antigens by mass photometry. (**A**) According to mass photometry analysis SARS-CoV-2 nucleocapsid protein (N) is a monomer with a mass of approximately 42 kDa. (**B**) Spike protein (alpha variant) (S) is mostly in monomeric state with a mass of approximately 124 kDa. Some S proteins have formed a tetramer with a mass of approximately 564 kDa. (**C**) Wuhan RBDmFc (RBD of original Wuhan strain with a fused mouse Fc fragment (mFc)) exists in multiple forms. Most of the proteins seem to be in dimer form (120 kDa) and some in tetrameric (244 kDa) and hexameric form (363 kDa). (**D**) Wuhan RBD without the Fc fragment is a monomer with a mass of approximately 34 kDa. (**E**) South Africa RBDmFc (RBD of beta strain with a fused mouse Fc fragment) exists similarly to Wuhan RBDmFc in multiple forms. Most of the proteins seem to be in dimer form (124 kDa) and some in tetrameric (248 kDa), hexameric (370 kDa) and octameric form (495 kDa). (**F**) South Africa RBD without the Fc fragment is a monomer with a mass of approximately 43kDa. (**G**) BA.4/5 RBDmFc (RBD containing the mutations from both the BA.4 and BA.5 subvariant of omicron strain fused with mouse Fc region) exists similarly to other RBDmFc proteins in multiple forms. Large part of the proteins seems to be in dimer form (125 kDa) and some in tetrameric (249 kDa) and octameric form (493 kDa). (**H**) BA.4/5 RBD without the Fc fragment is a monomer with a mass of approximately 36 kDa

Additional file 2: Supplementary Fig. 2A) administration route.

Through the subcutaneous route, the mice received either N or S protein alone or combined. Overall, the humoral immune response to the vaccine antigens increased with the successive doses. Already, after one dose the N-specific IgG levels were high in all the groups: GMTs ranging from 32254 to 57470 (Fig. 3B, Table 4). After the second dose the immune response was monitored for six weeks, during which a gradual increase in the GMTs was observed across all groups, with no evidence of a decline in response. At week 8 the response of the 4 + 4 µg vaccinated group was significantly lower than in those groups who received either solely 4 µg of N or the 8 + 8 µg vaccine, but this effect was not sustained throughout the immune response (Table 4). At later timepoints, co-administration frequently resulted in equal or higher N-specific titers compared with N alone. The increase in the amount of N to 8 µg in the vaccine containing solely N enhanced the elicited N-specific IgG levels significantly at week 10 when compared to groups containing 4 µg of N either alone or in combination with S. These findings suggest that any early antigen interference is transient and that co-delivery of S does not ultimately suppress N-specific humoral responses.

The S-specific IgG levels were quite low after the first immunization: GMTs ranging from 224 to 713 (Fig. 3C, Table 4). After the second vaccine dose, the S-specific IgG levels increased substantially and remained stable through the following period (until week 10). The S-specific IgG levels were lower than the N-specific IgG levels throughout the experiment (Table 4). The increase in the amount of S or the addition of N protein in the vaccine composition did not affect the elicited S-specific IgG levels significantly. Based on these results, the N protein seemed to be more immunogenic than the S protein. We concluded that decreasing the amount of N in the vaccine formulation for the next experiment should be done. We anticipated that the immune system may then elicit higher levels of antibodies against the S protein which contains the neutralizing epitopes. Based on the elicited S-specific IgG levels, doubling of the dosage of S did not significantly increase the IgG levels and, thus, we determined that 4 µg was the optimal dose. The safety profile of the vaccine was determined by monitoring the wellbeing of the mice by following their weight as well as behaviour daily by visual inspection. The vaccine formulations were well tolerated, and the body weights of the mice increased over time across all groups, and no adverse effects were observed during the study (see Additional file 3: Supplementary Fig. 3A).

Through the intranasal route, the mice received N protein combined with either the whole S or the wuRBDmFc protein (RBD from the original strain fused with mouse IgG2a Fc region). In the first preclinical experiment the intention was to pilot vaccinating via the intranasal immunization route. Therefore, due to ethical considerations the number of animals was kept low, and the results had no statistical significance. The used adjuvant AS04 is a parenteral adjuvant, but it has been experimented in an intranasal preclinical study previously [74]. Based on the results, we could determine that all the antigens elicited immune responses, but the variance between mice was high and we concluded that AS04 adjuvant is not optimal for mucosal immunizations. Antigen-specific immune responses remained negligible four weeks after the first dose. The N- and RBD-specific responses increased after the second dose and remained at that level for at least six weeks post-vaccination whereas S-specific responses remained negligible throughout the study (see Additional file 2: Supplementary Fig. 2B–D, respectively). Again, the N protein was more immunogenic when compared to RBD domain and the whole S protein (GMT range at termination 4032–10159 vs 3200–6400 and 400, respectively). The different doses of N did not significantly increase or decrease the N-specific IgG levels (see Additional file 2: Supplementary Fig. 2B) and, therefore, we determined that for the next experiment the N protein amount in the vaccine formulation could still be lowered. The RBD domain elicited higher IgG levels than the whole S protein (see Additional file 2: Supplementary Fig. 2C, D), although the dose of the whole S was 2 µg compared to the 4 and 8 µg of the wuRBDmFc protein. The doubling of the dose of wuRBDmFc did not increase the RBD-specific IgG levels significantly (see Additional file 2: Supplementary Fig. 2C) and, thus, we determined that 4 µg was the optimal dose. Although no significant differences were observed with

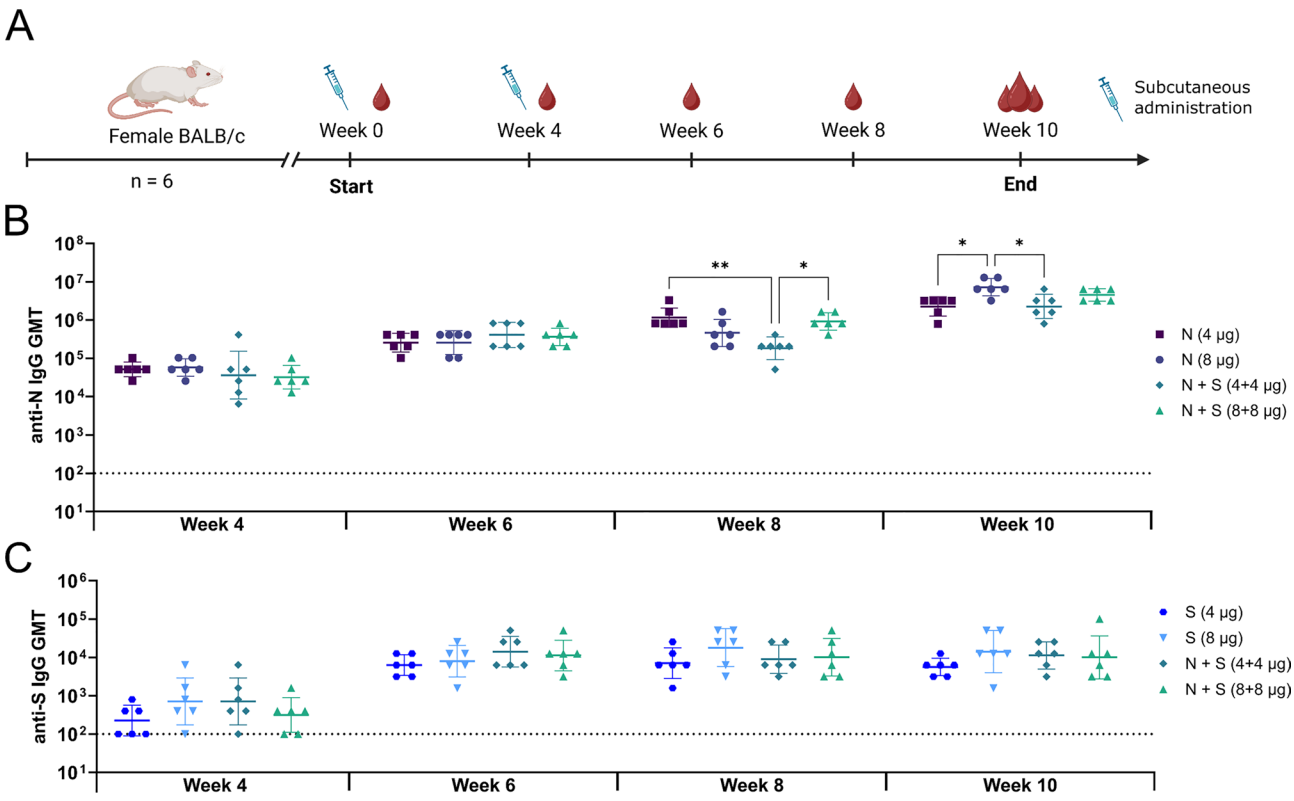

Fig. 3 Comparison of humoral immune responses following subcutaneous vaccination in mice. (**A**) Vaccination regimen for mice indicating the timepoints for immunizations and blood sampling. (B) Kinetics of S-specific and (**C**) N-specific total IgG endpoint titres depicted in serum measured with an ELISA assay. The results are expressed as geometric means with geometric standard deviations for the groups on Log10 scale. Significant differences between the groups are compared with Mann-Whitney U test or Kruskal-Wallis' test and Dunn's multiple comparison and are expressed as $*p < 0.05$ and $**p < 0.01$. Undetectable antibody titres are denoted with a titre of 100 and represented as a dotted line

Table 4 Antigen-specific IgG GMTs during different timepoints

Antigen	Time-point (week)	Geometric mean titres			
		4 µg N	**8 µg N**	**4 µg N + 4 µg S**	**8 µg N + 8 µg S**
N	4	51 200	57 470	36 204	32 254
	6	258 032	258 032	409 600	364 912
	8	1 158,524	459 760	182 456	919 521
	10	2 262,742	7 183,757	2 262,742	4 525,483
		4 µg S	**8 µg S**	**4 µg N + 4 µg S**	**8 µg N + 8 µg S**
S	4	224	713	713	317
	6	6 400	8 063	14 368	11 404
	8	7 184	18 102	9 051	10 159
	10	5 702	14 368	11 404	10 159

the intranasal administration route, these results demonstrated that wuRBDmFc and N antigens can be taken up by immune cells via intranasal route without priming with parenteral immunisation. However, two doses were not enough to achieve robust immune response after intranasal immunisation. Immunisation through intranasal route was well-tolerated and the body weights of the mice increased over time in all groups, and no health issues were observed during the study (see Additional file 3: Supplementary Fig. 3B).

Nucleocapsid protein enhances RBD- and S-specific humoral and cellular immune responses in mice

Based on the results of the pilot study, we concluded that optimal immunogenicity may require an additional booster vaccination intranasally. Therefore, in the following preclinical study we increased the number of immunizations from two to three and further optimized the vaccine formulations by adjusting the antigen dose and modifying the adjuvant. Groups 1–4 received three vaccine doses intranasally, while group 5 received the first dose subcutaneously, followed by two intranasal doses to see if parenteral priming enhances the immune responses (Fig. 4A). Since there are no mucosal adjuvants that have EMA or FDA approval for human use, branched polyethylenimine (BPEI) was tested as an adjuvant in all groups. BPEI is a branched isoform of PEI which is an organic polycation used as nucleic acid transfection reagents in vitro, and gene and DNA vaccine delivery vehicles in vivo [75, 76]. In previous studies, BPEI has been showed to possess adjuvant properties when administered intranasally [53, 54] and parenterally [77].

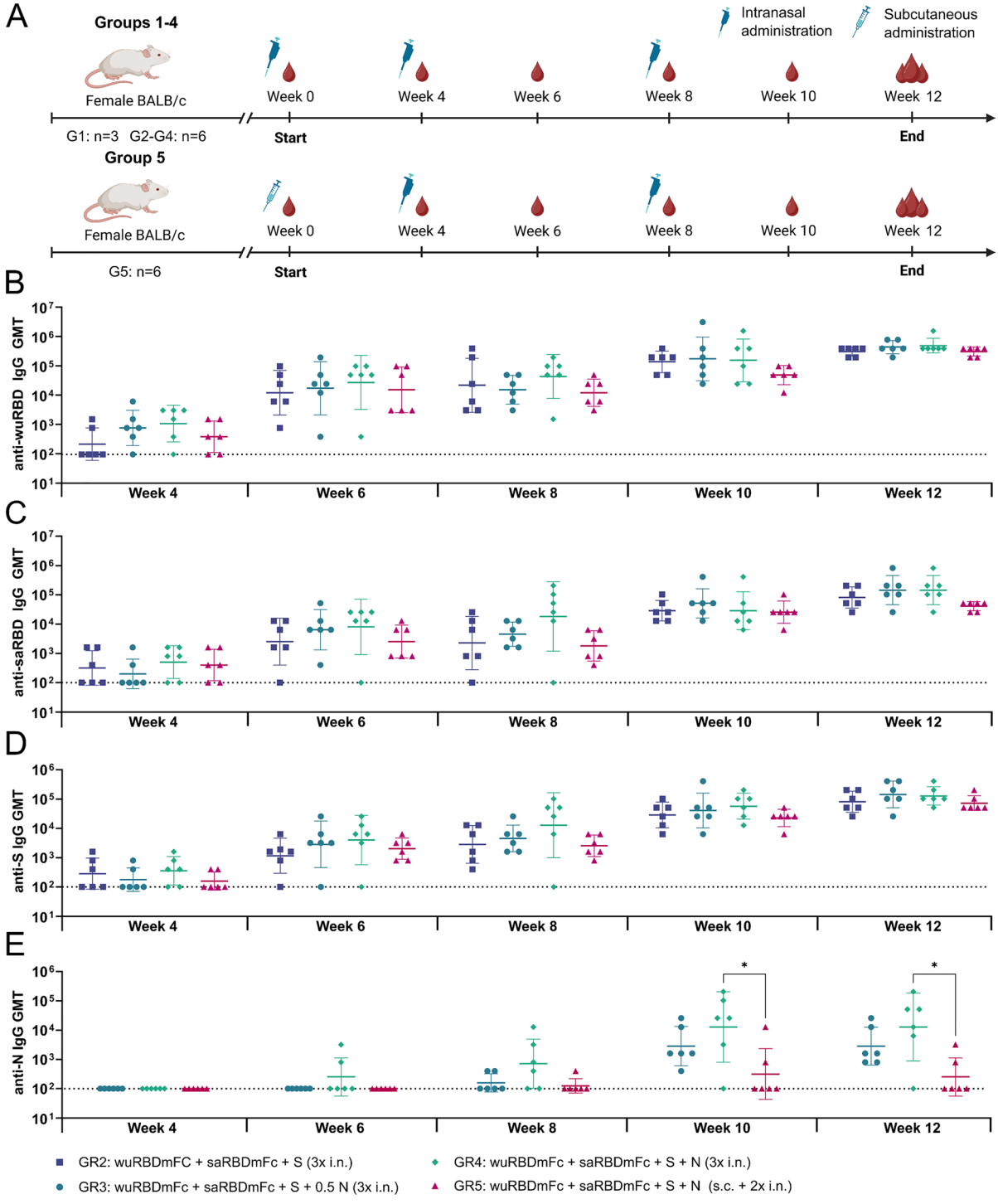

Fig. 4 Comparison of humoral immune responses following different vaccination regimens in mice. (**A**) Vaccination regimen for groups 1–4 and for group 5. (**B**) Kinetics of wuRBD-specific, (**C**) saRBD-specific, (**D**) S-specific and (**E**) N-specific total IgG endpoint titres from serum measured with an ELISA assay. The results are expressed as geometric means with geometric standard deviations for the groups on Log10 scale. Significant differences compared with Kruskal-Wallis' test and Dunn's multiple comparison are expressed as $*p < 0.05$. Undetectable antibody titres are denoted with a titre of 100 and represented as dotted line. wuRBD stands for RBD from the original "Wuhan" strain and saRBD for RBD from the beta "South Africa" strain

Table 5 Antigen specific serum IgG geometric mean titres at different timepoints

		Geometric mean titres		
Antigen	**Timepoint (week)**	**Group 2**	**Group 3**	**Group 4**
wuRBD	4	224	800	1131
	6	12 800	18 102	28 735
	8	22 807	16 127	45 614
	10	144 815	182 456	162 550
	12	325 100	459 760	516 064
saRBD	4	317	200	504
	6	2 540	6 400	8 063
	8	2 263	4 525	18 102
	10	28 735	51 200	28 735
	12	81 275	144 815	144 815
S	4	283	178	356
	6	1 164	2 851	4 032
	8	2 851	4 525	12 800
	10	28 735	40 637	57 470
	12	81 275	144 815	129 016

Overall, the humoral immune responses progressively increased with each antigen dose. At the termination after three vaccine doses, the levels of wuRBD-, saRBD- and S-specific immune responses were comparable across all vaccination groups (Fig. 4B–D). Moreover, the development of immune responses against wuRBD, saRBD and S proteins was similar throughout the study, indicating that the choice of vaccine antigen among these three did not influence the humoral immune response elicited by the vaccine. Interestingly, the inclusion of N protein at low doses in the vaccine formulation appeared to enhance the generation of wuRBD-, saRBD-, and S-specific immune responses. Groups 3 and 4, which received 0.5 µg or 1 µg of N protein, respectively, showed consistently higher, although not statistically significant, IgG levels throughout the study compared to group 2, which did not receive N in the vaccine formulation (Table 5). At termination, wuRBD-specific responses of groups 3 and 4 were 1.4-fold and 1.6-fold higher, respectively, than the response of group 2. Similarly, the saRBD-specific responses of groups 3 and 4 were 1.8-fold higher and the S-specific responses 1.8-fold and 1.6-fold higher, respectively, than the responses of group 2. Furthermore, the administration route appears to have substantial effect especially on the N-specific immune response (Fig. 4E), which is consistently lower in group 5 which received the first dose subcutaneously compared to group 4. Overall, the N-specific IgG levels were lower in this study compared to the pilot study (Fig. 3B, Supplementary Fig. 2B and Fig. 4E).

The polarization of the immune response was evaluated by assessing IgG subtype IgG_1 and IgG_{2A} responses from termination serum samples. The IgG_{2A} levels, indicative of Th1-associated responses, were higher in all groups compared to the corresponding IgG_1 levels, which are associated with Th2-type immunity (Fig. 5A,B, Table

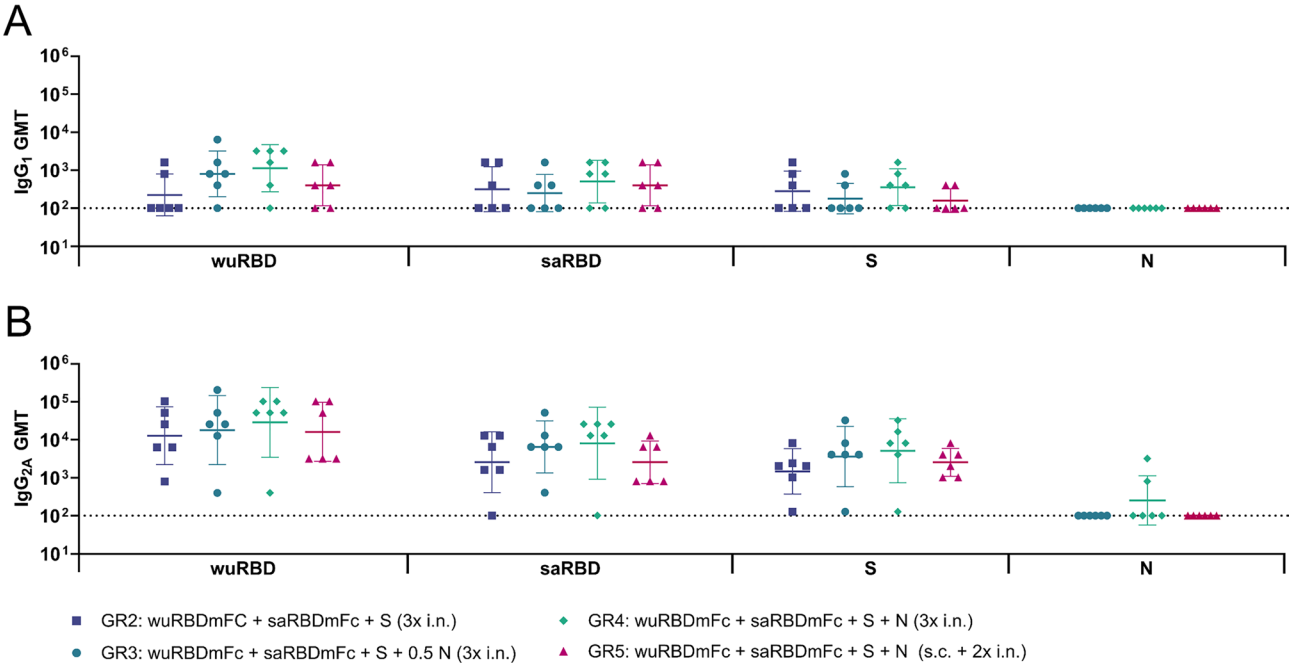

Fig. 5 Subtype IgG levels of vaccinated mice. (**A**) IgG_1 and (**B**) IgG_{2A} endpoint titres at termination (week 12) measured with an ELISA assay. The results are expressed as geometric means with geometric standard deviations for the groups on Log10 scale. Significant differences were compared with Kruskal-Wallis' test and Dunn's multiple comparison. Undetectable antibody titres are denoted with a titre of 100 and represented as dotted line. wuRBD stands for RBD from the original "Wuhan"strain and saRBD for RBD from the beta "South Africa" strain

Table 6 Antigen-specific IgG_1:IgG_{2A} ratios for each vaccination group

Antigen	Group	Geometric mean titres		
		IgG_1	IgG_{2A}	IgG_1:IgG_{2A} ratio
wuRBD	2	224	12 800	0.018
	3	800	18 102	0.044
	4	1 131	28 735	0.039
	5	400	16 127	0.025
saRBD	2	317	2 540	0.125
	3	252	6 400	0.039
	4	504	8 063	0.063
	5	400	2 540	0.016
S	2	283	1 164	0.243
	3	178	2 851	0.062
	4	356	4 032	0.088
	5	159	2 016	0.079
N	3	Not detected	Not detected	Not applicable
	4	Not detected	252	Not applicable
	5	Not detected	Not detected	Not applicable

Ratios over 1 indicate a Th1 biased response and ratios under 1 suggest a Th2 biased response. Value Not detected means no response was observed in ELISA assays. Value Not applicable means that IgG_1:IgG_{2A} ratio could not be calculated due to one or both responses being below the detection limit

6). The findings, thus, indicate a Th1-dominant immune response to the whole S protein and the RBDmFc proteins. No N-specific IgG1 response could be detected and only group 4 elicited a weak N-specific IgG2a response (Fig. 5A,B, Table 6). The vaccine formulation was well-tolerated, the mice showing consistent weight gain throughout the study (see Additional file 3: Supplementary Fig. 3C).

Mucosal immune responses were analysed from bronchoalveolar lavage (BAL) samples collected at the termination by measuring the antigen-specific IgA and IgG levels by ELISA. wuRBDmFc and saRBDmFc antigens were able to elicit IgA antibodies to some extent: GMTs ranging from 21.6 to 50.4 and 10.4 to 35.6 respectively, but N- and S-specific responses remained negligible (Fig. 6A) indicating that N and S proteins were likely not as effectively taken up by antigen presenting cells as Fc-conjugated antigens. The IgA level in BAL samples was the highest in group 3 (GMT for wuRBD 50.4 and for saRBD 35.6). IgG levels in BAL samples were quite similar to IgA levels with the exception that N and S proteins were also able to elicit IgG antibodies to some extent (Fig. 6B). Based on these results it seems that a very low dose of N might boost the mucosal immune responses against RBD antigens, but further studies are needed to confirm this finding.

To measure T cell responses from the vaccinated mice, the secretion of IL-2, IFN-γ, and TNF was analysed from isolated mouse splenocytes following stimulation with vaccine antigens using FluoroSpot assay. IL-2 secretion was the most robust, particularly after stimulation with both RBD proteins, where responses were observed across all vaccination groups (Fig. 7A). Notably, a significant IL-2 response was also detected in group 3 after stimulation with S and N proteins whereas the response of other groups was negligible. In contrast, IFN-γ responses were less pronounced (Fig. 7B). However, a notable response following stimulation with both RBD proteins was observed in group 3, while responses

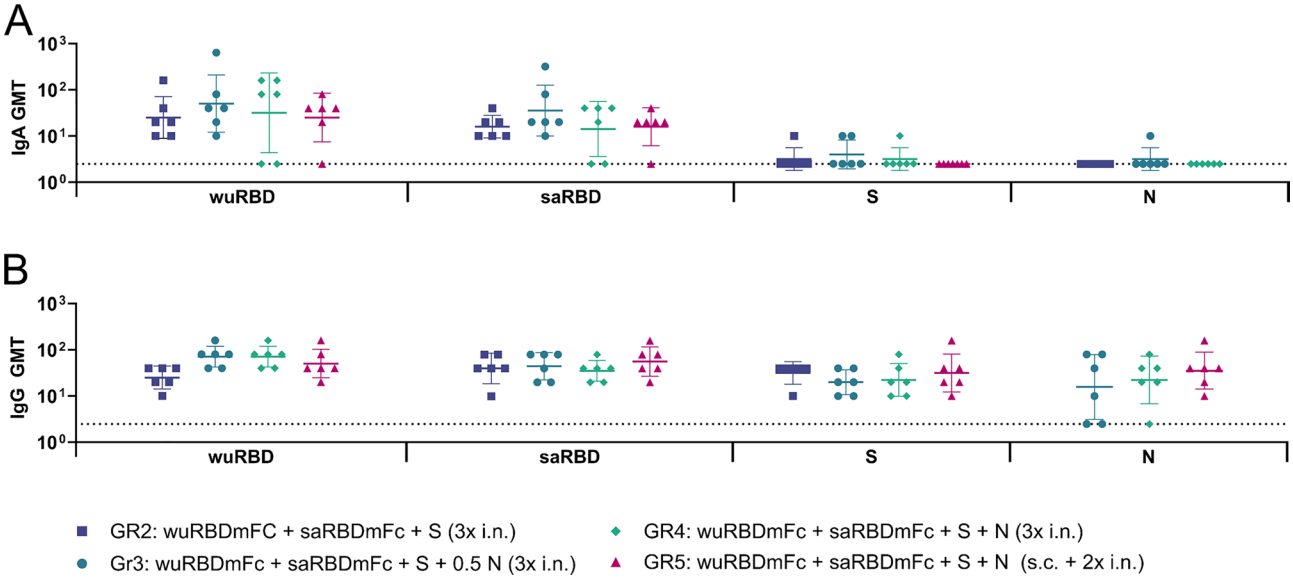

Fig. 6 Mucosal immune responses in bronchoalveolar lavage samples collected upon termination. (**A**) Antigen-specific IgA and (**B**) IgG endpoint titres from bronchoalveolar lavage samples measured with an ELISA assay. The results are expressed as geometric means with geometric standard deviations for the groups on Log10 scale. Significant differences were compared with Kruskal-Wallis' test and Dunn's multiple comparison. Undetectable antibody titres are denoted with a titre of 2.5 and represented as dotted line. wuRBD stands for RBD from the original strain and saRBD for RBD from the beta strain

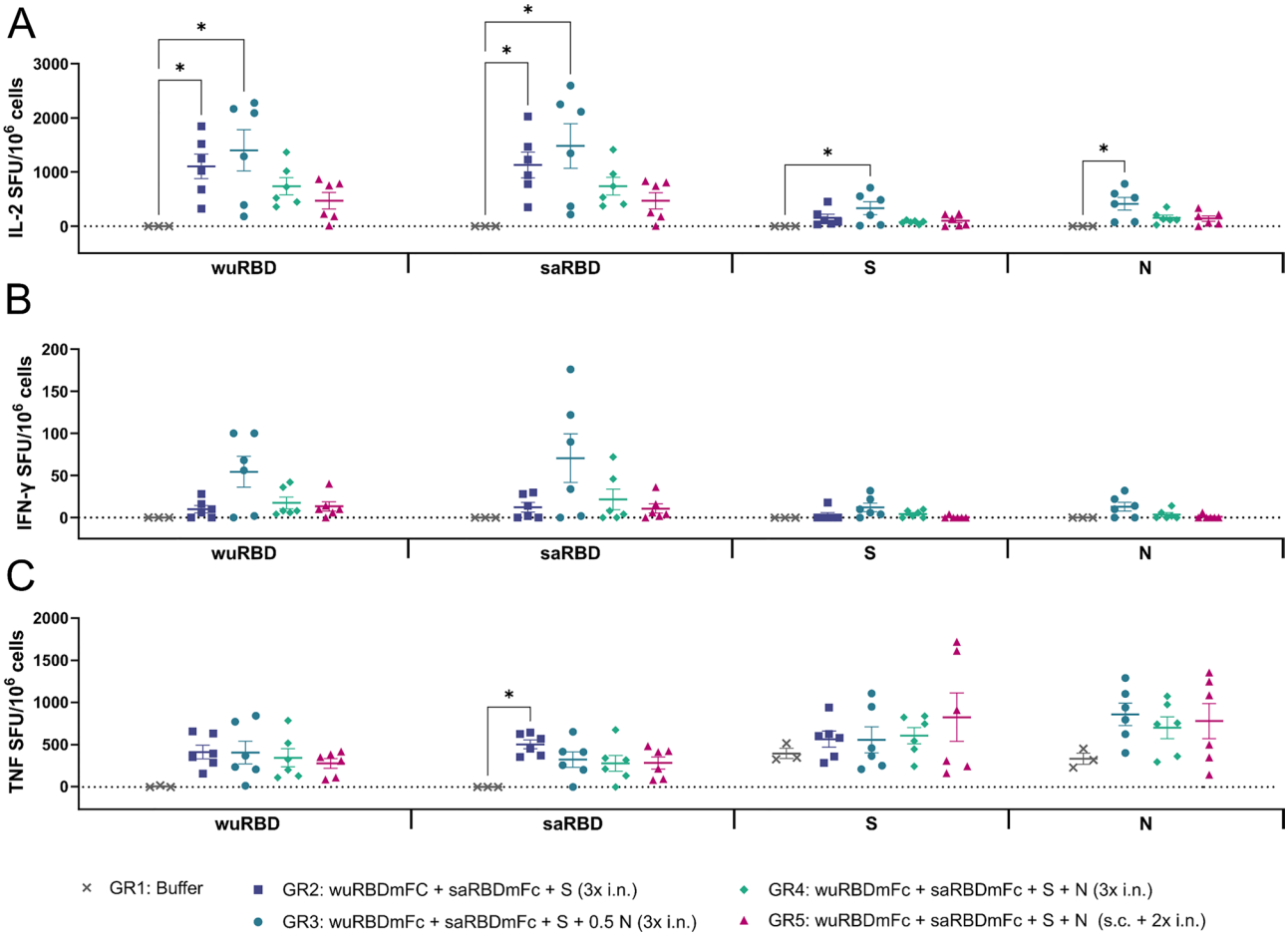

Fig. 7 Cellular immune response. The secretion of (**A**) IL-2, (**B**) IFN-γ and (**C**) TNF from isolated mouse splenocytes after stimulation with vaccine antigens. The results are expressed as arithmetic means of responding cells which are expressed as the number of spot-forming units/106 splenocytes with standard errors of mean for the groups. Significant differences between buffer and vaccination groups are compared with Kruskal-Wallis' test and Dunns' multiple comparison and expressed as $*p < 0.05$. wuRBD stands for RBD from the original "Wuhan" strain and saRBD for RBD from the beta "South Africa" strain

in other groups and after stimulation with S or N proteins were negligible. When analysing the secretion of IL-2 and IFN-γ the addition of 0.5 µg of N in the vaccine composition seemed to boost cellular immune responses against both RBD domains as the numbers of spot forming units (SFU) per million cells were higher in group 3 than in group 2 when stimulating with wuRBD domain (IL-2: arithmetic mean 1399 vs 1105 and IFN-γ: arithmetic mean 54 vs 10) and saRBD domain (IL-2: arithmetic mean 1481 vs 1130 and IFN-γ: arithmetic mean 71 vs 12) (Fig. 7A,B). Interestingly, stimulation with S or N proteins led to substantial TNF secretion, even in the buffer control group (Fig. 7C). This suggests the presence of some non-specific TNF production, potentially linked to innate immune cell activation.

Intramuscular priming followed by intranasal vaccination improves N- and RBD-specific humoral, cellular, and mucosal immune responses in mice

Based on the results of the second study, we wanted to further investigate the possible booster effect of the N protein and to see whether intramuscular priming enhances the immune responses more than subcutaneous priming. Groups 1–3 received all three doses intranasally, while group 4 and 5 received the first dose intramuscularly, followed by two intranasal doses (Fig. 8A). Additionally, three mice from each vaccination group (groups 2–5) were followed up for an additional eight weeks to see whether the humoral immune response stayed stable and whether the cellular immune response would improve over time.

Overall, the humoral immune responses progressively increased with each successive dose. Already after the first intramuscularly administered dose, both the BA.4/5RBD- and N-specific IgG levels were high and significantly higher than the levels elicited by intranasal

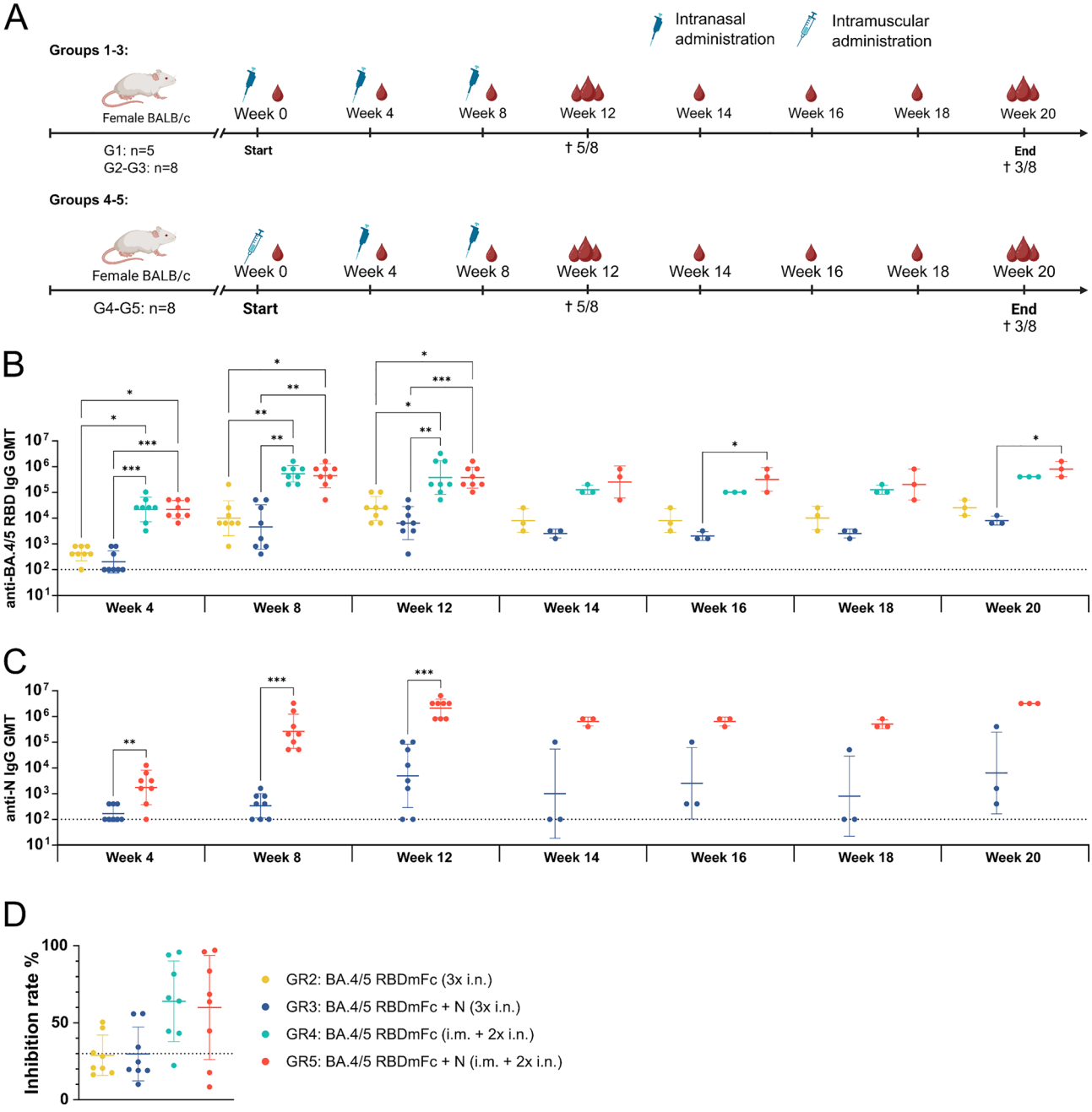

Fig. 8 Comparison of humoral immune responses following different vaccination regimens in mice. (**A**) Vaccination regimens for groups 1–3 and groups 4–5. Groups 2–5 initially contained 8 mice per group. 5 animals per group were terminated at week 12 for endpoint analyses and a subset of 3 mice per group were followed up for an additional 8 weeks to assess the durability and kinetics of antibody responses. (**B**) Kinetics of BA0.4/5 RBD-specific and (**C**) N-specific total IgG endpoint titres from serum measured with an ELISA assay. The results are expressed as geometric means with geometric standard deviations for the groups on Log10 scale. Significant differences between groups are compared with mann-whitney U test or Kruskal-Wallis' test and Dunn's multiple comparison and are expressed as $*p < 0.05$, $**p < 0.01$, and $***p < 0.001$. Undetectable antibody titres are denoted with a titre of 100 and represented as dotted line. (**D**) neutralizing antibodies determined with a commercial ELISA kit. The neutralization ability of the antibodies was measured against the SARS-CoV-2 omicron subvariant BA.4/5. Percentual inhibition rate was calculated for each mouse. Neutralization effect was deemed to present if inhibition rate was 30% or over. The dotted line presents 30% inhibition in the assay. The results are expressed as arithmetic means with standard deviations for each group. BA.4/5 RBD stands for RBD containing the mutations from both the BA.4 and BA.5 subvariant of omicron strain

Table 7 BA.4/5-specific IgG geometric mean titres during different timepoints

Antigen	Timepoint (week)	Geometric mean titres			
		Group 2	Group 3	Group 4	Group 5
BA.4/5 RBD	4	200	436	21 527	21 527
	8	9 870	4 525	531 185	446 672
	12	23 475	6 400	375 605	375 605
	14	8 063	2 540	129 016	258 032
	16	8 063	2 016	102 400	325 100
	18	10 159	2 540	129 016	204 800
	20	25 600	8 063	409 600	819 200

administration (Fig. 8B,C). After the second dose, IgG levels kept increasing and a similar statistically significant difference was seen between the different immunization schemes as after the first dose. After the third dose, RBD-specific antibody levels did not increase anymore and actually decreased in the intramuscularly vaccinated groups. N-specific antibody levels instead kept increasing substantially. Similar statistical difference was still seen between the different immunization schemes as after the first and second dose. The addition of N in the vaccine compositions did not seem to boost or significantly decrease the RBD-specific IgG responses during weeks 0–12 in any of the groups (Table 7). During the 8-week follow-up period, both the RBD- and N-specific antibody levels first weakly decreased but then stayed approximately at the same level. During this period group 5 had consistently higher IgG levels than group 4 (on average 2.2-fold higher), indicating that the N booster effect might still be effective (Fig. 8B, Table 7).

The neutralization ability of the vaccine-induced antibodies was analysed with a commercial neutralizing antibody ELISA kit. In the intranasally primed groups (groups 2 and 3) the neutralizing effect was mostly negligible (Fig. 8D). In the intramuscularly primed groups (groups 4 and 5) most of the mice had neutralizing antibodies. One mouse in group 4 and two mice in group 5 did not reach the inhibition rate (IR) of 30%, which deemed the neutralizing effect to be present. The IR ranged from 22 to 96%, the mean being 64% in group 4, and from 8 to 97% the mean being 60% in group 5.

The polarization of the immune response was evaluated by assessing IgG subtype IgG_1 and IgG_{2A} responses from termination serum samples (Fig. 9A–D). When evaluating both the RBD- and N-specific IgG_1 levels the intramuscularly primed groups had higher IgG_1 levels than the intranasally primed groups (Fig. 9A,C, Table 8). During the 8-week follow-up period, the levels stayed consistent and did not decline. In addition, a weak N booster effect could also be seen in the intramuscularly primed groups (GMT at week 20 for group 4,479,032 and group 5,650,199) (Fig. 10A). RBD-specific IgG_{2A}

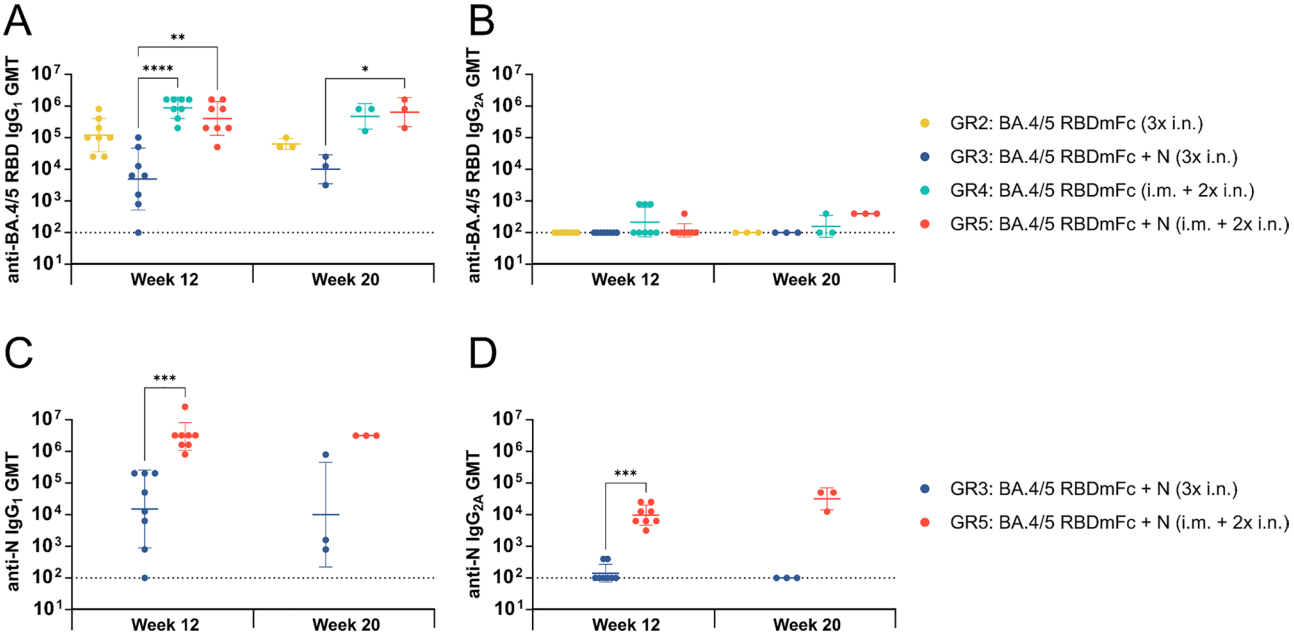

Fig. 9 Subtype IgG levels of vaccinated mice. (**A**) IgG1 and (**B**) IgG2A endpoint titres at termination (week 12 and 20) measured with an ELISA assay. The results are expressed as geometric means with geometric standard deviations for the groups on Log10 scale. Significant differences between groups are compared with mann-whitney U test or Kruskal-Wallis' test and Dunn's multiple comparison and are expressed as $*p<0.05$, $**p<0.01$, $***p<0.001$ and $****p<0.0001$. Undetectable antibody titres are denoted with a titre of 100 and represented as dotted line. BA.4/5 RBD stands for RBD containing the mutations from both the BA.4 and BA.5 subvariant of omicron strain. BA.4/5 RBD stands for RBD containing the mutations from both the BA.4 and BA.5 subvariant of omicron strain

Table 8 Antigen-specific IgG1:IgG2a ratios for each vaccination group

Antigen	Time-point (week)	Group	Geometric mean titres		
			IgG_1	IgG_{2A}	IgG_1:IgG_{2A} ratio
BA.4/5 RBD	12	2	121 775	Not detected	Not applicable
		3	4 935	Not detected	Not applicable
		4	893 344	218	4 098
		5	409 600	119	3442
BA.4/5 RBD	20	2	64 508	Not detected	Not applicable
		3	10 159	Not detected	Not applicable
		4	479 032	159	3013
		5	650 199	400	1625
N	12	3	15 222	141	108
		5	3 004839	9 870	304
N	20	3	10 159	Not detected	Not applicable
		5	3 276,800	32 254	102

Ratios over 1 indicate a Th1 biased response and ratios under 1 suggest a Th2 biased response. Value Not detected means no response was observed in ELISA assays. Value Not applicable means that IgG_1:IgG_{2A} ratio could not be calculated due to one or both responses being below the detection limit

responses were practically non-existent for all groups (Fig. 9B, Table 8). However, an IgG_{2A} response was seen with group 5 when measuring the N-specific responses (Fig. 9D, Table 8). The intramuscularly primed group 5 had significantly higher levels of IgG_{2A} antibodies than the intranasally primed group 3. The group 5's IgG_{2A} levels even increased substantially in the 8-week follow up period (GMT at week 129,870 and at week 2,032,254). All in all, these findings and the calculated IgG_1:IgG_{2A} ratios indicate a clearly Th2-dominant immune response to all vaccine antigens (Table 8).

Overall, based on the serum total IgG and subtype IgG results, intramuscular priming seems to enhance the humoral immune response significantly compared to intranasal and subcutaneous priming. Intramuscular priming also improves the neutralization ability of the antibodies. With both immunization schemes, the vaccine formulations were well tolerated. The body weights of the mice increased over time across all groups, and no adverse effects were observed during the study (see Additional file 3: Supplementary Fig. 3D,E).

Mucosal immune responses were determined from BAL samples by measuring IgA and IgG levels with ELISA. Both RBD- and N-specific IgA levels were non-existent when the vaccines were administered solely intranasally (Fig. 11A, B). RBD-specific IgA levels were significantly higher with intramuscularly primed groups (groups 4 and 5) at week 12 when compared to intranasally primed groups (groups 2 and 3). At week 20 the levels were still substantially higher in groups 4 and 5 than in groups 2 and 3, but the differences were not statistically significant. During the 8 week follow-up period, the RBD-specific IgA levels declined more rapidly than the RBD-specific BAL or serum IgG levels (Figs. 11A, C and 8B). The N-specific IgA levels also declined during the follow-up period, but less rapidly than the RBD-specific response (Fig. 11B). When analysing the mucosal IgG response, a similar significant difference was observed between the different immunization schemes as with IgA response. Groups 4 and 5 had significantly higher IgG levels in their BAL samples than group 3 at week 12 (Fig. 11C). Similar difference was observed at week 20, but it was not statistically significant. A weak N booster effect could also be observed when analysing the RBD-specific mucosal IgG levels. Both at week 12 and 20, group 5 had somewhat higher GMTs than group 4 (160 vs 139 and 160 vs 64). During the follow up period, the RBD-specific mucosal IgG levels declined to negligible levels in groups 2 and 3 but remained similar to week 12 responses in groups 4 and 5 (Fig. 11C). The N-specific mucosal IgG levels slightly increased in group 5 (GMT 735 vs 806) and declined in group 3 (GMT 17 vs 8) (Fig. 11D).

The secretion of IL-2, IFN-γ, and TNF was analysed from isolated mouse splenocytes following stimulation with vaccine antigens using FluoroSpot assay to measure the T cell responses. Like previously, IL-2 secretion was the most robust, particularly after stimulation with the RBD protein where responses were observed across all vaccination groups (Fig. 10A). Notably, at week 12 a significant IL-2 response was also detected in group 5 after stimulation with N protein and the vaccine of the group (combination of RBDmFc and N) whereas the response of group 4 was mild (Fig. 10B,C). At week 20 the IL-2 responses had increased in all groups with group 5 clearly standing out. The inclusion of N protein in the vaccine composition and priming intramuscularly clearly improves the IL-2 response elicited by the vaccine. Group 5 consistently had the highest mean SFU/10^6 cells values within every stimulation and time point. In contrast, IFN-γ responses were less pronounced (Fig. 10D–F). Still, group 5 stood out once again. At week 12 when stimulating with RBD (Fig. 10D) or a combination of RBD and N (Fig. 10F) a significant IFN-γ response was detected in group 5. At week 20 these responses had increased and were higher than those seen in other groups. When stimulating with N, IFN-γ response in group 5 was higher than that in group 3 but the differences were statistically not significant (Fig. 10E). It seems that intramuscular priming enhances the IFN-γ response when compared to intranasally primed groups. Additionally, when the N protein was included in the vaccine regimen that led to a higher IFN-γ production level upon antigen stimulation

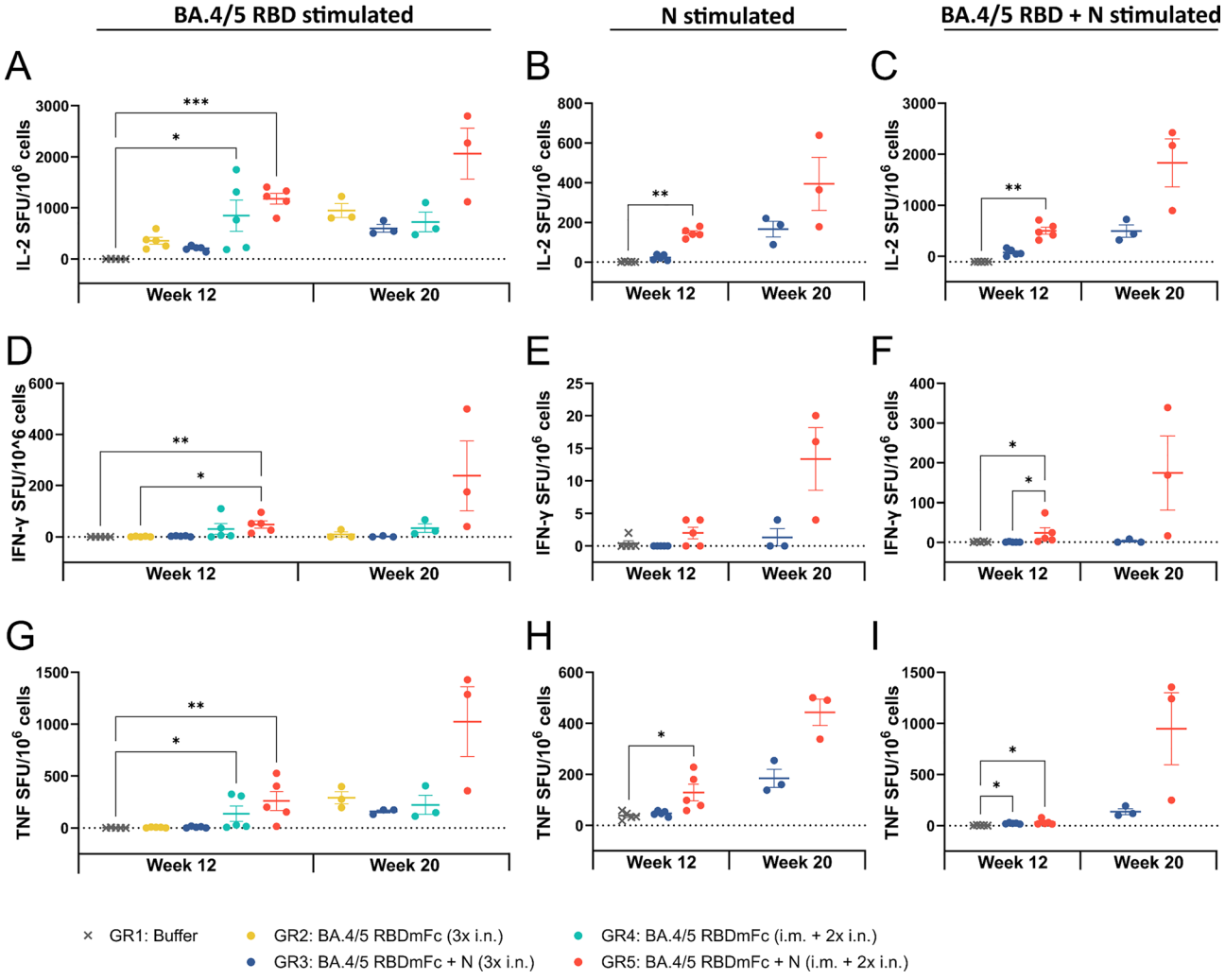

Fig. 11 Cellular immune responses measured by FluoroSpot assay. The secretion of IL-2, IFN-γ and TNF measured from isolated mouse splenocytes after stimulation with BA.4/5 RBD (**A**, **D**, **G**), N (**B**, **E**, **H**) and a combination of BA.4/5 RBD and N (**C**, **F**, **I**). The results are expressed as arithmetic means with standard errors of the means for each group. Significant differences between groups are compared with Mann-Whitney U test or Kruskal-Wallis' test and Dunn's multiple comparison and are expressed as $*p < 0.05$, $**p < 0.01$, and $***p < 0.001$. BA0.4/5 RBD stands for RBD containing the mutations from both the BA.4 and BA.5 subvariant of omicron strain

(group 5 vs. group 4). In the solely intranasally vaccinated groups IFN-γ response was not detected at week 12 or 20. In turn, TNF responses across all groups were more pronounced than IFN-γ responses, but less robust than IL-2 responses (Fig. 10G–I). When stimulating splenocytes with RBD, the responses of intranasally primed groups 2 and 3 were negligible at week 12 but increased considerably to week 20 (at week 12 mean SFU/10^6 cells GR2 4 and GR3 7 vs. at week 20 GR2 290 and GR3 159) (Fig. 10G). With intramuscularly primed groups 4 and 5 the TNF responses were significant already at week 12 (mean SFU/10^6 cells GR4 138 and GR5 263) and kept increasing to week 20 (mean SFU/10^6 cells GR4 222 and GR5 1024) (Fig. 10G). Interestingly, stimulation with N protein again led to a moderate TNF secretion even in the buffer control group (Fig. 10H). This suggests the presence of some non-specific TNF production, potentially derived from insect cell culture and linked to innate immune cell activation. The responses in groups 4 and 5 were prominent and increased during the follow up period (at week 12 mean SFU/10^6 cells GR4 47 and GR5 128 vs. at week 20 GR4 184 and GR5 443). Stimulation with the vaccine (combination of RBD and N) did not elicit a TNF response from the buffer control group but significant responses were detected with groups 4 and 5 (Fig. 10I). Once again, the responses enhanced by week 20. The increase of the response was substantially higher in group 5 compared to that in group 4 (at week 12 mean SFU/10^6 cells GR4 22 and GR5 32 vs. at week 20 GR4 137 and GR5 949) indicating once again the importance of intramuscular priming and the inclusion of N in the vaccine composition. Overall, based on the cellular response

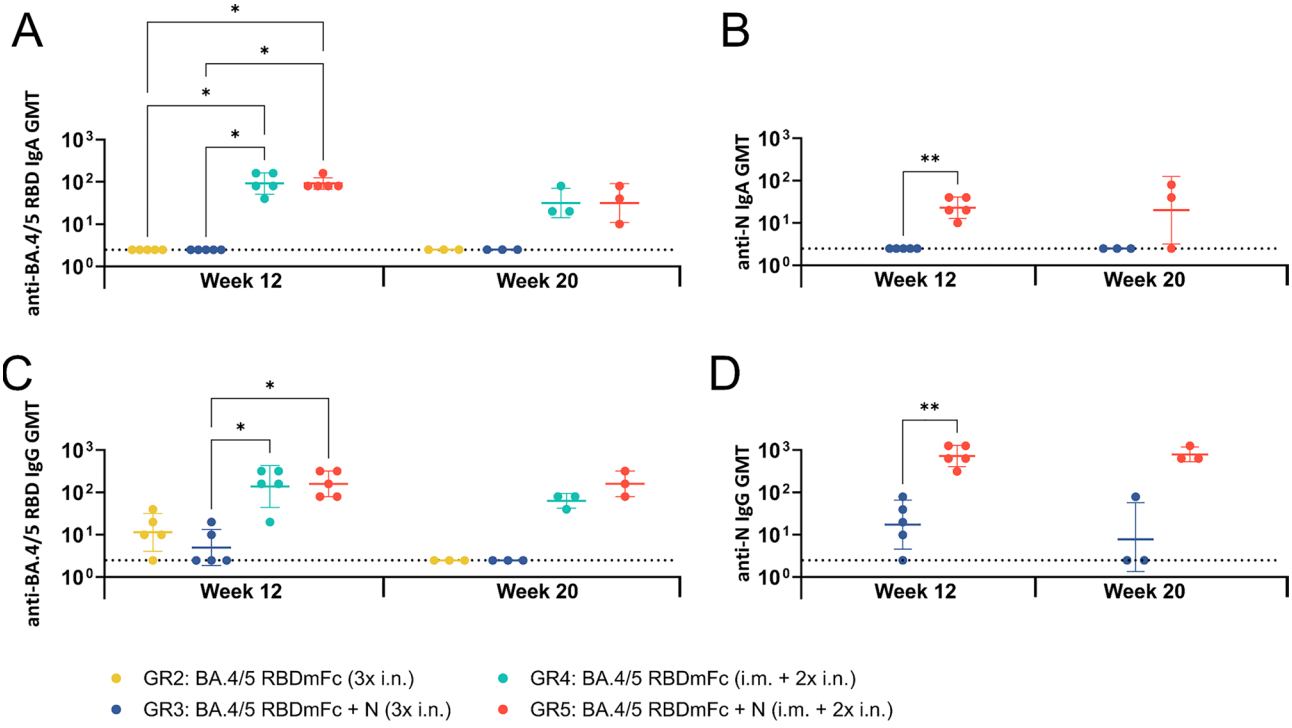

Fig. 10 Mucosal immune responses in bronchoalveolar lavage samples collected upon termination. (**A**) BA.4/5 RBD-specific and (**B**) N-specific IgA and (**C**) BA.4/5 RBD-specific and (**D**) N-specific IgG endpoint titres depicted in bronchoalveolar lavage measured with an ELISA assay. The results are expressed as geometric means with geometric standard deviations for the groups on Log10 scale. Significant differences between groups are compared with Mann-Whitney U test or Kruskal-Wallis' test and Dunn's multiple comparison and are expressed as $*p < 0.05$ and $**p < 0.01$. Undetectable antibody titres are denoted with a titre of 2.5 and represented as dotted line. BA0.4/5 RBD stands for RBD containing the mutations from both the BA.4 and BA.5 subvariant of omicron strain

data intramuscular priming and the inclusion of N in the vaccine composition boost the RBD-specific IL-2, IFN-γ, and TNF responses substantially.

Discussion

SARS-CoV-2 coronavirus was first identified in late 2019 in Wuhan, China, and shortly thereafter WHO declared COVID-19 as a public health emergency of international concern [3, 78]. The development of the first vaccines against COVID-19 was unprecedentedly fast and within the first year from the identification of the virus several manufacturers had already obtained market authorization for their vaccines. As of February 2024, at least 64 COVID-19 vaccines are approved by one or more national regulatory authorities [79] and according to WHO over 380 vaccine candidates are in clinical or pre-clinical development phase [14]. These vaccines rely on diverse platforms including inactivated viruses, mRNA, DNA, recombinant proteins and viral vectors. Most target the S protein or its RBD domain. Although estimates of annual global deaths from COVID-19 have declined by up to 95% compared with the early stages of the pandemic, the disease continues to pose a major public health challenge, with as many as two million new infections occurring each year [80].

Although currently available COVID-19 vaccines are highly effective in preventing severe disease, their ability to block infection or viral transmission is comparatively limited. This is evident from the continued spread of SARS-CoV-2 within populations with high vaccination coverage, particularly following the emergence of new variants [81, 82]. Persistent community transmission and ongoing viral replication facilitate the evolution of additional variants that can partially evade existing immune responses, thereby reducing the capacity of current vaccines to prevent infection and symptomatic illness [82–85]. Therefore, annual booster doses are needed to maintain protection. WHO has been forced to establish a Technical Advisory Group on COVID-19 Vaccine Composition (TAG-CO-VAC) which assesses the public health implications of emerging SARS-CoV-2 variants on the performance of COVID-19 vaccines and issues timely recommendations on proposed modifications to vaccine antigen composition. WHO releases statements on the antigen composition of COVID-19 vaccines every six months. Thus, in the worst-case scenario manufacturers should be able to update their vaccine compositions and produce a new vaccine batch every six months. Therefore, new solutions must be invented. It remains essential to enhance the protective efficacy of vaccines, diminish

viral shedding and transmission, and strengthen the capacity of vaccines to confer robust immunity against newly emerging variants of pathogenic agents.

Vaccines that induce a durable mucosal immune response localized in the respiratory tract have the potential to prevent SARS-CoV-2 infection, replication, and shedding and therefore, transmission [81]. Recent investigations have demonstrated that tissue-resident memory T cells (TRM cells) within mucosal tissues play a critical role in mediating long-term protection against mucosal pathogens [86, 87]. During SARS-CoV-2 infection, TRM cells are induced in the lungs of patients with both mild and severe disease and can persist for up to 10 months, indicating their potential contribution to sustained mucosal immunity [88, 89]. Furthermore, T cell epitopes have been shown to remain highly conserved between the Wuhan and Omicron strains [90, 91]. In contrast, many neutralizing antibody epitopes are located in variable regions of the S protein, and mutations within the RBD domain of viral variants diminish the neutralizing capacity of antibodies elicited by ancestral vaccine sequences [92]. Because viral variants are more adept at evading antibody responses than T cell responses, vaccines capable of inducing both robust T cell immunity and antibody production, particularly within the respiratory tract, may offer substantial advantages. In addition, the induction of mucosal IgA following vaccination appears to contribute importantly to protection against SARS-CoV-2 infection, particularly at the respiratory mucosa [29]. Furthermore, targeting mucosal-associated invariant T (MAIT) cells in protein-based SARS-CoV-2 vaccines represents a promising approach to enhance local immunity. MAIT cells, which are abundant in the respiratory mucosa, can be activated by cytokine-driven or MR1-dependent pathways to rapidly produce antiviral cytokines and cytotoxic mediators [93–95]. Incorporation of adjuvants capable of stimulating MAIT cells could therefore potentiate mucosal immune activation and complement adaptive immune responses [96, 97]. Thus, vaccines that elicit both mucosal antibodies and strong T cell responses may provide a broader and longer-lasting protection against SARS-CoV-2.

In this study we aimed to develop a protein-based SARS-CoV-2 vaccine capable of inducing broad protection based on mucosal antibodies and T cell responses. We sought to tackle these aims by testing different protein compositions for the vaccine candidates and different immunization schemes. The whole S protein or its RBD domain are the most common immunogens in the approved SARS-CoV-2 vaccines [79]. The choice is natural as full length S protein, its S1 subunit, and the RBD domain are the most immunogenic antigens found in CoVs and the main targets for neutralizing antibodies [6]. Nevertheless, the COVID-19 pandemic made it clear that the variable regions in S are highly mutation-prone leading to immune evasion and, thus, decreased vaccine efficacy and long-term protection [85, 98]. Thus, our proposed solution was to include either S or several different RBD domains in the vaccine or N protein together with S and/or RBD domain(s).

It has been previously proposed that mixing vaccines from different SARS-CoV-2 strains may induce better cellular and humoral immune responses and lead to a better immunity against emerging variants compared with homologous vaccination [99]. This hypothesis has also been tested by combining key immunogens from different SARS-CoV-2 strains into a single protein subunit vaccine. Xu and coworkers developed Wuhan – Beta and Delta-Omicron RBD-dimer vaccines [100]. Both chimeric protein subunit vaccines elicited broader responses to SARS-CoV-2 variants and better neutralizing antibody responses against variants compared to homodimers [100]. Another chimeric vaccine was developed by Liang et al. [101]. They constructed a mutation-integrated trimeric form of RBDs from Wuhan, Beta and Kappa strains and detected that it induced significantly higher titres of neutralizing antibody responses against the Beta and Delta variants than a homotrimer constructed from the Wuhan strain alone [101]. Additionally, both Cohen et al. [102] and Walls et al. [103] constructed mosaic nanoparticle immunogens, in which multivalent RBDs from various coronavirus were co-displayed on the same particle surface. Owing to the high-dense and heterotypic arrays of the antigens, this mosaic nanoparticle-type vaccine candidate elicited much stronger and broader antibody responses compared with the monomeric immunogen. It was also immunogenically superior to the homotypic RBD nanoparticles [102, 103]. RBD domain itself alone is a quite small immunogen (approx. 28.5kDa). To improve its immunogenicity as a vaccine candidate, researchers have also utilized Fc engineering where RBD is fused to an IgG Fc fragment. The Fc fragment has a natural ability to form dimers and, thus, fusing an RBD domain to an Fc fragment creates RBD dimer structures. Compared to monovalent immunogens, bivalent Fc-fused immunogens may be able to elicit more robust B-cell responses by triggering cross-linking of B-cell receptors [104]. Additionally, Fc fusion aids in transportation across the airway [48], prolongs the half-life of the antigen [49] and facilitates efficient antigen uptake, processing and presentation to T cells [42–45]. Previously Fc-fused protein vaccines have been developed against MERS, SARS, and H5N1 influenza A viruses and researchers have found that Fc-fused proteins are more immunogenic than those lacking the fused Fc domain [56, 105, 106]. During COVID-19 pandemic Fc fusion constructs have also been utilized in the vaccine development against SARS-CoV-2 [31, 53, 107–111]. In the latest study by Zhang and

colleagues they showed that RBD-Fc was able to more efficiently reach the lungs of mice and attain better retention in both nasal cavity and lungs compared to a bivalent RBD without Fc [110].

In the present study, we aimed to compare the immunogenicity of the stabilized S protein (produced in insect cells) to the immunogenicity of RBDmFc proteins (produced in mammalian cells). It is known that SARS-CoV-2 S protein is heavily glycosylated [112–114] and approximately 40% of the protein surface is shielded by glycans [115]. Although insect cells are not able to produce as complex glycosylation patterns as mammalian cells, we chose to produce the stabilized S protein in High Five insect cells as insect cells are used in the production of several recombinant protein and virus-like particle-based vaccine candidates, (such as influenza [116], Japanese encephalitis [117] and Zika virus [118]) and, therefore, have demonstrated efficiency and scalability especially for vaccine development. Nevertheless, we observed the Fc-fused RBD domains to be more immunogenic than the whole S protein. This finding may be caused by the Fc fusion and the multimerization of the RBD constructs. We observed that RBDmFc fusion proteins form dimers and even oligomers such as tetramers, hexamers, and even octamers. Here the low immunogenicity of S protein might also be due to the insect cell-produced S protein forming primarily monomers instead of the trimeric form encountered in the native virus although it contains the trimerization domain. The glycosylation pattern produced by the High Five insect cells could also have an impact on the low immunogenicity of the whole S protein. S protein is a highly glycosylated protein [112–115] and the glycosylation pattern affects the elicited humoral immune responses [119]. In addition, we observed that including a low dose of N protein in the vaccine composition boosted both the RBD- and S-specific humoral, mucosal, and cellular immune responses. Furthermore, there are several other advantages in including the N protein in the vaccine composition. N protein has been considered as a promising target for vaccine-induced immune responses [120–128]. It is highly conserved [121, 129] and a prominent target of SARS-CoV-2 specific T-cell responses during COVID-19 [130, 131]. Although N protein is located inside the mature virions, during infection it is expressed in virus-infected cells [132, 133] and exposed on their membranes [134, 135] facilitating targeting and elimination by cytotoxic T cells [136, 137] and natural killer cells [138–140]. In addition, Le Bert and colleagues have also demonstrated that previously infected SARS-CoV patients possess long lasting memory T cells which are reactive to N protein over 17 years after the SARS epidemic in 2003 [141]. N-based subunit vaccines have been previously evaluated in preclinical or clinical studies either alone [121–123, 126] or in combination with S or M protein [120, 124, 125, 127, 128] and found to provide potent immunogenicity and a strong protective effect involving T cells and other non-neutralizing effector mechanisms. In accordance with these previous studies [120–128], we also observed N protein to be extremely immunogenic. In addition, we also found out that the N-specific IgA responses waned slower than the RBD-specific IgA responses (Fig. 11B). Interestingly, we found that the inclusion of N in the vaccine increased the RBD-specific IgG and IgA levels as well as splenocyte IL-2 and IFN-γ secretion (Figs. 4B, C, 6A, B and 7A, B).

Alongside antigen selection, the immunization route proved a crucial determinant for the quality of the immune response. The majority of approved vaccines or those in clinical or pre-clinical development phase rely on intramuscular administration [14, 79] which induces high levels of systemic IgG antibodies, but little mucosal IgG and dimeric IgA antibodies [28–31] which are crucial in promoting protective immunity against SARS-CoV-2 [29]. Secretory, polymeric IgA can neutralize incoming viral particles at mucosal surfaces before the infection of epithelial cells takes place, which is important for an optimal protection against respiratory virus infections [142]. In the present study we sought to induce mucosal IgA antibodies by vaccinating the mice through the intranasal route. In addition to solely vaccinating intranasally, we also tested immunization schemes which combined either subcutaneous or intramuscular priming with subsequent intranasal boosting. According to our observations, subcutaneous priming followed by intranasal boosting elicited the lowest humoral and cellular immune responses. Vaccinating solely through the intranasal route produced variable mucosal responses. In the second study we obtained RBD-specific mucosal IgA responses from mice that had solely been vaccinated intranasally. However, in the third experiment these responses were not detectable. The explanation to these different responses might lie also in the vaccine composition. In the second experiment the vaccine candidates contained a whole S protein and additionally RBD domains from two different variants when in turn in the third experiment the candidates contained only a single RBD domain from omicron variant BA0.4/5. Previous studies have stated that multivalent or chimeric antigens elicit stronger immune responses than homomers [100, 101]. Combining intramuscular priming with intranasal boosting proved to be a superior immunization scheme. Previously, Mao and coworkers and Lapuente and coworkers have both come to the same conclusion in their respective studies [32, 143]. This strategy enhanced the systemic and mucosal immune responses significantly compared to intranasal vaccination. Also, based on the cellular response data intramuscular priming

and the inclusion of the N protein in the vaccine composition boosted the RBD-specific IL-2, IFN-γ, and TNF responses substantially (Fig. 10). Mechanistically, recent work by Kwon et al. [144] suggests that intranasal delivery of unadjuvanted protein antigens elicits robust mucosal IgA responses primarily when preceded by parenteral priming, which enables recall of pre-existing systemic immune memory at mucosal sites rather than de novo induction. In this context, intramuscular priming may generate memory B-cell populations that can be recruited to the respiratory mucosa upon intranasal boosting and differentiate into IgA-secreting plasma cells, providing a potential explanation for the reduced efficiency of homologous intranasal immunization in inducing durable mucosal IgA responses.

A major limitation of this study is the absence of viral challenge or transmission-relevant experiments, which precludes assessment of whether the observed systemic and mucosal immune responses translate into protection against infection, disease, or transmission. In addition, the predominance of Th2-skewed immune responses observed in the third study requires careful interpretation. S-based SARS-CoV-2 vaccines typically elicit Th1-leaning immunity, and the second study where S and several RBDs were administered alone or in combination with N showed a more balanced or weakly Th1-biased responses. In contrast, the formulations of BA.4/5 RBDmFc protein + N protein and BA.4/5 RBDmFc protein alone generated a stronger Th2 profile than anticipated. The basis for this shift is not fully understood but may reflect formulation-specific factors such as antigen ratios or the immunological properties of the protein–adjuvant combinations used here. Importantly, strongly Th2-biased responses have been associated in some reports with enhanced morbidity following SARS-CoV-2 infection, underscoring the need to determine whether the immune profiles observed in this study are protective in vivo. These uncertainties limit interpretation of the immunogenicity data and highlight the need for follow-up studies incorporating optimized antigen dosing, additional adjuvant conditions, and in vivo efficacy models.

Together, the results demonstrate that Fc-fused RBD constructs are highly immunogenic, the inclusion of N enhances both antibody and T cell responses, and intramuscular priming followed by intranasal boosting represented the most effective delivery scheme tested. These findings support the development of multicomponent, heterologous vaccination strategies that combine variant RBDs with conserved antigens such as N, administered in ways that maximize both systemic and mucosal immunity. Nevertheless, further work is still needed to screen a broader panel of adjuvants to identify those capable of more effectively enhancing mucosal antibody production and T cell–mediated responses. In addition, future studies incorporating viral challenge models will be essential to determine whether the immune profiles elicited by these formulations translate into meaningful protection against infection, disease, or transmission.

Conclusions

In summary, our results demonstrate that inclusion of the SARS-CoV-2 N protein in vaccine formulations containing RBD or S enhances both humoral and cellular immune responses against the RBD and whole S antigens in mice. While repeated intranasal administration elicited progressively increasing antibody responses, intramuscular priming followed by intranasal boosting proved superior in generating robust and durable systemic and mucosal immunity. The addition of the N protein in the vaccine formulation with RBD domain or S protein increased RBD- and S-specific IgG responses, supported the induction of mucosal antibodies, and enhanced cellular immunity as detected by an increased IL-2 and IFN-γ secretion. Importantly, the combination of intramuscular priming with N protein-containing formulations elicited the highest magnitude and breadth of T cell responses, as well as neutralizing antibodies, highlighting the synergistic effects of antigen selection and immunization route. All vaccine regimens were well tolerated, indicating a favourable safety profile of the vaccines. Together, these findings suggest that incorporating N into RBD-based vaccines and employing a heterologous prime-boost strategy may improve both the quality and durability of protective immunity, offering a promising approach for next-generation vaccine development against SARS-CoV-2 variants and possibly other emerging coronaviruses with pandemic potential.

Abbreviations

RBD	Receptor binding domain
S	Spike protein
N	Nucleocapsid protein
BPEI	Branched polyethylenimine
AS04	Adjuvant system 04
IgG	Immunoglobulin G
IgA	Immunoglobulin A
COVID-19	Coronavirus disease 2019
CoV	Coronavirus
HCoV	Human coronavirus
SARS-CoV	Severe acute respiratory syndrome coronavirus
MERS-CoV	Middle East respiratory syndrome coronavirus
WHO	World Health Organisation
SARS-CoV-2	Severe acute respiratory syndrome coronavirus 2
E	Envelope protein
M	Membrane protein
FDA	U.S. Food and Drug Administration
EMA	European Medicines Agency
BRM cells	Tissue-resident memory B cells
TRM cells	Tissue-resident memory T cells
Fc	Fragment, crystallizable
Ig	Immunoglobulin
FcγR	Fc-gamma receptor
APC	Antigen-presenting cell

TCR	T cell receptor
ADCC	Antibody-dependent cellular cytotoxicity
ADCP	Antibody-dependent cellular phagocytosis
FcRn	Neonatal Fc receptor
PAMP	Pathogen-associated molecular pattern
CT	Cholera toxin
LT	Heat-labile toxin
dmLT	Double mutant detoxified version of the heat-labile enterotoxin
mmCT	Non-toxic multiple mutant of cholera toxin
PRR	Pattern recognition receptor
TLR	Toll-like receptor
ODN	Oligodeoxynucleotide
Poly(I:C)	Polyinosinic-polycytidylic acid
ISCOM	Immune-stimulating complex
MOI	Multiplicity of infection
TFF	Tangential flow filtration
PBS	Phosphate buffered saline
RT	Room temperature
RBDmFc	Receptor binding domain genetically fused to a mouse IgG_{2A} Fc fragment
s.c.	Subcutaneously
i.n.	Intranasally
wuRBDmFc	Receptor binding domain from the original "Wuhan" strain genetically fused to a mouse IgG_{2A} Fc fragment
saRBDmFc	Receptor binding domain from the beta strain (B0.1.351, first identified in South Africa) genetically fused to a mouse IgG_{2A} Fc fragment
BAL	Bronchoalveolar lavage
i.m.	Intramuscularly
ELISA	Enzyme-linked immunosorbent assay
HRP	Horseradish peroxidase
OPD	o-Phenylenediamine
GMT	Geometric mean titre
PC	Positive control
NC	Negative control
IR	Inhibition rate
mAb	Monoclonal antibody
MPLA	Monophosphoryl lipid A
SFU	Spot forming unit
TAG-CO-VAC	Technical Advisory Group on COVID-19 Vaccine Composition

Supplementary Information

The online version contains supplementary material available at https://doi.org/10.1186/s12879-026-12634-x.

Supplementary Material 1

Acknowledgements

The technical assistance and guidance given by Niklas Kähkönen, Janne Kärnä, Merja Jokela, Ulla Kiiskinen and Niina Ikonen (Tampere University) is gratefully acknowledged. We would like to thank Emilia Löfblom, Jenni Hirvonen and Mariia Stasyk (Tampere Vocational College Tredu) for their help in performing the immunological analyses. Additionally, we would like to thank Rolle Rahikainen (Protein Nanosystems, Tampere University) for technical assistance and guidance with the mass photometry experiments. Tampere University Preclinical Facility and its personnel are thanked for providing equipment and assistance for this study. In addition, we acknowledge Biocenter Finland for infrastructure support.

Author contributions

MMH conceived the original idea for the project. MMH and SG developed the idea together into the final research plan. MMH designed the nucleocapsid protein and spike protein constructs. OR, MAR, RAN and PK designed the RBDmFc constructs. MMH, SG, AI, AP, RAN and MAR produced, purified, and characterized the vaccine antigens. MMH and SG designed the immunological analyses and MMH, SG, SS, IM and VL performed immunizations, terminations, and sampling of the mice. SG, HL, SP and EH performed ELISA assays and SG and HL the analyses. SG and SS performed the FluoroSpot assays and analyses. SG performed the neutralization assay and the analysis. LK, IJ and PK provided reagents, discussed and interpreted the data. SG, MMH and HL drafted the manuscript and figures. IM produced the graphical abstract under the supervision of SG and MMH. All authors discussed the results and commented on the manuscript. All authors read and approved the final manuscript.

Funding

Open access funding provided by Tampere University (including Tampere University Hospital). The research was funded by Business Finland Research to Business -funding (MMH, SG, HL), Finnish Cultural Foundation (grant number #50221563, MMH, HL, SG), Research Council of Finland (grant numbers #335870 and #355414, MMH), The Jane and Aatos Erkko Foundation (grant numbers #3067-84b53 and #5360-cc2fc, IJ), Tampere University graduate school (SG, SS, VL), Tampere Tuberculosis Foundation (MMH, SG, HL, VL), The Research Foundation of the Pulmonary Diseases (SG), The Foundation of Onni and Hilja Tuovinen (SG), Finnish Society for Study of Infectious Diseases (SG), Tampere Science Foundation (SG), The Finnish Medical Foundation (grant number: 5106, RAN), the Biomedicum Helsinki Foundation (grant number: 20220219, RAN) and Nordic SARS Response AB (RAN, MAR, AP). The funders played no role in study design, data collection, analysis and interpretation of data, or the writing of this manuscript.

Data availability

The datasets used and/or analysed during this study are available from the corresponding author on reasonable request.

Declarations

Ethics approval

All animal experiments in this study were carried out following the Finnish Act on the Protection of Animals Used for Scientific or Educational Purposes (497/2013) and the National Institutes of Health guidelines for laboratory animal care. Procedures were approved by the Regional State Administrative Agency, Pirkanmaa, Finland (decision number ESAVI/1408/2021). All animal reporting was conducted in accordance with ARRIVE guidelines. All efforts were made to minimize animal suffering and to reduce the number of animals used. The welfare of the animals was monitored throughout the experiment. Separate ethics committee or IRB approval for animal work is not applicable under Finnish regulations.

Competing interests

MMH, SG and HL are inventors in a pending patent application FI 20253474 (Immunogenic composition and uses thereof). Based on the Act on the Right in Inventions in Finland, all authors employed by Tampere University have given all rights to the University and, thus, no competing interests exist. RAN, MAR and AP developed the wuRBD-mFc-8his antigen, and they own equity in Nordic SARS Response AB that holds sole ownership and commercialization rights of the wuRBD-mFc-8his cDNA (GenBank ID: PP599180.1) and its derivates used in this study. The remaining authors declare no competing interests.

Author details

[1]Virology and Vaccine Immunology, Faculty of Medicine and Health Technology, Tampere University, Tampere, Finland
[2]Department of Physiology, Faculty of Medicine, University of Helsinki, Helsinki, Finland
[3]Nordic SARS Response AB, Stockholm, Sweden
[4]School of Engineering Sciences in Chemistry, Biotechnology and Health, KTH Royal Institute of Technology, Stockholm, Sweden
[5]Institute of Biomedicine, Faculty of Medicine, University of Turku, Turku, Finland
[6]Clinical Microbiology, Turku University Hospital, Turku, Finland
[7]InFlames Research Flagship Center, University of Turku, Turku, Finland

Received: 21 November 2025 / Accepted: 16 January 2026
Published online: 29 January 2026

References

1. Perlman S, Masters PS. Coronaviridae: the viruses and their replication. In: Howley PM, Knipe DM, editors. Fields virology: emerging viruses. 7th. Philadelphia, UNITED STATES: Wolters Kluwer Health; 2020 [cited 2023 Jan 12]. p. 986–1073. Available from: http://ebookcentral.proquest.com/lib/tampere/detail.action?docID=6676894.
2. Summary of probable SARS cases with onset of illness from 1 November 2002 to 31 July 2003. [cited 2024 May 16]. Available from: https://www.who.int/publications/m/item/summary-of-probable-sars-cases-with-onset-of-illness-from-1-november-2002-to-31-july-2003.
3. Wu F, Zhao S, Yu B, Chen YM, Wang W, Song ZG, et al. A new coronavirus associated with human respiratory disease in China. Nature. 2020;579(7798):265–69.
4. Coronavirus disease (COVID-19) - World Health Organization. [cited 2024 May 16]. Available from: https://www.who.int/emergencies/diseases/novel-coronavirus-2019.
5. Hu B, Guo H, Zhou P, Shi ZL. Characteristics of SARS-CoV-2 and COVID-19. Nat Rev Microbiol. 2021;19(3):141–54.
6. Walls AC, Park YJ, Tortorici MA, Wall A, McGuire AT, Structure VD. Function, and antigenicity of the SARS-CoV-2 spike glycoprotein. Cell. 2020;181(2):281–92. e6.
7. Li YD, Chi WY, Su JH, Ferrall L, Hung CF, Wu TC. Coronavirus vaccine development: from SARS and MERS to COVID-19. J Biomed Sci. 2020;27(1):104.
8. Du L, Tai W, Zhou Y, Jiang S. Vaccines for the prevention against the threat of MERS-CoV. Expert Rev Vaccines. 2016;15(9):1123–34.
9. Du L, He Y, Zhou Y, Liu S, Zheng BJ, Jiang S. The spike protein of SARS-CoV - a target for vaccine and therapeutic development. Nat Rev Microbiol. 2009;7(3):226–36.
10. Wang N, Shang J, Jiang S, Du L. Subunit vaccines against emerging pathogenic human coronaviruses. Front Microbiol. 2020;11:298.
11. He YX, Zhou YS, Siddiqui P, Niu JK, Jiang SB. Identification of immunodominant epitopes on the membrane protein of the severe acute respiratory syndrome-associated coronavirus. J Clin Microbiol. 2005;43(8):3718–26.
12. Zheng N, Xia R, Yang C, Yin B, Li Y, Duan C, et al. Boosted expression of the SARS-CoV nucleocapsid protein in tobacco and its immunogenicity in mice. Vaccine. 2009;27(36):5001–07.
13. Liu SJ, Leng CH, Lien SP, Chi HY, Huang CY, Lin CL, et al. Immunological characterizations of the nucleocapsid protein based SARS vaccine candidates. Vaccine. 2006;24(16):3100–08.
14. WHO. COVID-19 vaccine tracker and landscape. [cited 2025 Apr 17]. Available from: https://www.who.int/publications/m/item/draft-landscape-of-covid-19-candidate-vaccines.
15. COVID-19 medicines | European Medicines Agency (EMA). [cited 2025 Apr 24]. Available from: https://www.ema.europa.eu/en/human-regulatory-overview/public-health-threats/coronavirus-disease-covid-19/covid-19-medicines.
16. Comirnaty | European Medicines Agency (EMA). 2020 [cited 2025 Apr 24]. Available from: https://www.ema.europa.eu/en/medicines/human/EPAR/comirnaty.
17. Kostaive | European Medicines Agency (EMA). 2025 [cited 2025 Apr 24]. Available from: https://www.ema.europa.eu/en/medicines/human/EPAR/kostaive.
18. Nuvaxovid | European Medicines Agency (EMA). 2021 [cited 2025 Apr 24]. Available from: https://www.ema.europa.eu/en/medicines/human/EPAR/nuvaxovid.
19. Spikevax (previously COVID-19 Vaccine Moderna) | European Medicines Agency (EMA). 2021 [cited 2025 Apr 24]. Available from: https://www.ema.europa.eu/en/medicines/human/EPAR/spikevax.
20. Jeyanathan M, Afkhami S, Smaill F, Miller MS, Lichty BD, Xing Z. Immunological considerations for COVID-19 vaccine strategies. Nat Rev Immunol. 2020;20(10):615–32.
21. Tang J, Zeng C, Cox TM, Li C, Son YM, Cheon IS, et al. Respiratory mucosal immunity against SARS-CoV-2 after mRNA vaccination. Sci Immunol. 2022;7(76):eadd4853.
22. Lund FE, Randall TD. Scent of a vaccine. Science. 2021;373(6553):397–99.
23. Szabo PA, Miron M, Farber DL. Location, location, location: tissue resident memory T cells in mice and humans. Sci Immunol. 2019;4(34):eaas9673.
24. Allie SR, Bradley JE, Mudunuru U, Schultz MD, Graf BA, Lund FE, et al. The establishment of resident memory B cells in the lung requires local antigen encounter. Nat Immunol. 2019;20(1):97–108.
25. Laczkó D, Hogan MJ, Toulmin SA, Hicks P, Lederer K, Gaudette BT, et al. A single immunization with nucleoside-modified mRNA vaccines elicits strong cellular and humoral immune responses against SARS-CoV-2 in mice. Immunity. 2020;53(4):724–32.e7.
26. Goel RR, Painter MM, Apostolidis SA, Mathew D, Meng W, Rosenfeld AM, et al. mRNA vaccines induce durable immune memory to SARS-CoV-2 and variants of concern. Science. 2021;374(6572):abm0829.
27. Turner JS, O'Halloran JA, Kalaidina E, Kim W, Schmitz AJ, Zhou JQ, et al. SARS-CoV-2 mRNA vaccines induce persistent human germinal centre responses. Nature. 2021;596(7870):109–13.
28. Israelow B, Mao T, Klein J, Song E, Menasche B, Omer SB, et al. Adaptive immune determinants of viral clearance and protection in mouse models of SARS-CoV-2. Sci Immunol. 2021;6(64):eabl4509.
29. Sheikh-Mohamed S, Isho B, Chao GYC, Zuo M, Cohen C, Lustig Y, et al. Systemic and mucosal IgA responses are variably induced in response to SARS-CoV-2 mRNA vaccination and are associated with protection against subsequent infection. Mucosal Immunol. 2022;15(5):799–808.
30. Sano K, Bhavsar D, Singh G, Floda D, Srivastava K, Gleason C, et al. SARS-CoV-2 vaccination induces mucosal antibody responses in previously infected individuals. Nat Commun. 2022;13(1):5135.
31. Li W, Wang T, Rajendrakumar AM, Acharya G, Miao Z, Varghese BP, et al. An FcRn-targeted mucosal vaccine against SARS-CoV-2 infection and transmission. Nat Commun. 2023;14(1):7114.
32. Mao T, Israelow B, Peña-Hernández MA, Suberi A, Zhou L, Luyten S, et al. Unadjuvanted intranasal spike vaccine elicits protective mucosal immunity against sarbecoviruses. Science. 2022;378(6622):eabo2523.
33. Li X, Wang L, Liu J, Fang E, Liu X, Peng Q, et al. Combining intramuscular and intranasal homologous prime-boost with a chimpanzee adenovirus-based COVID-19 vaccine elicits potent humoral and cellular immune responses in mice. Emerg Microbes Infect. 2022;11(1):1890–99.
34. Hassan AO, Kafai NM, Dmitriev IP, Fox JM, Smith BK, Harvey IB, et al. A single-dose intranasal ChAd vaccine protects Upper and lower respiratory tracts against SARS-CoV-2. Cell. 2020;183(1):169–84.e13.
35. Hassan AO, Feldmann F, Zhao H, Curiel DT, Okumura A, Tang-Huau TL, et al. A single intranasal dose of chimpanzee adenovirus-vectored vaccine protects against SARS-CoV-2 infection in rhesus macaques. Cell Rep Med. 2021;2(4):100230.
36. Bricker TL, Darling TL, Hassan AO, Harastani HH, Soung A, Jiang X, et al. A single intranasal or intramuscular immunization with chimpanzee adenovirus-vectored SARS-CoV-2 vaccine protects against pneumonia in hamsters. Cell Rep. 2021;36(3):109400.
37. Fischer RJ, van Doremalen N, Adney DR, Yinda CK, Port JR, Holbrook MG, et al. ChAdOx1 nCoV-19 (AZD1222) protects Syrian hamsters against SARS-CoV-2 B.1.351 and B.1.1.7. Nat Commun. 2021;12(1):5868.
38. van Doremalen N, Purushotham JN, Schulz JE, Holbrook MG, Bushmaker T, Carmody A, et al. Intranasal ChAdOx1 nCoV-19/azd1222 vaccination reduces viral shedding after SARS-CoV-2 D614G challenge in preclinical models. Sci Transl Med. 2021;13(607):eabh0755.
39. Sui Y, Kar S, Chawla B, Hoang T, Yu Y, Wallace SM, et al. Adjuvanted subunit intranasal vaccine reduces SARS-CoV-2 onward transmission in hamsters. Front Immunol. 2025;16:1514845.
40. Tobias J, Steinberger P, Wilkinson J, Klais G, Kundi M, Wiedermann U. SARS-CoV-2 vaccines: the advantage of mucosal vaccine delivery and local immunity. Vaccines. 2024;12(7):795.
41. Park SC, Wiest MJ, Yan V, Wong PT, Schotsaert M. Induction of protective immune responses at respiratory mucosal sites. Hum Vaccines Immunother. 2024;20(1):2368288.
42. Regnault A, Lankar D, Lacabanne V, Rodriguez A, Théry C, Rescigno M, et al. Fcgamma receptor-mediated induction of dendritic cell maturation and major histocompatibility complex class I-restricted antigen presentation after immune complex internalization. J Exp Med. 1999;189(2):371–80.
43. Ravetch JV, Bolland S. IgG Fc receptors. Annu Rev Immunol. 2001;19:275–90.
44. Nimmerjahn F, Ravetch JV. Fcγ receptors as regulators of immune responses. Nat Rev Immunol. 2008;8(1):34–47.
45. Junker F, Gordon J, Qureshi O. Fc gamma receptors and their Role in antigen uptake, presentation, and T cell activation. Front Immunol. 2020;11. https://www.frontiersin.orghttps://www.frontiersin.org/journals/immunology/articles/10.3389/fimmu.2020.01393/full.
46. Spiekermann GM, Finn PW, Ward ES, Dumont J, Dickinson BL, Blumberg RS, et al. Receptor-mediated immunoglobulin G transport across mucosal barriers in adult life: functional expression of FcRn in the mammalian lung. J Exp Med. 2002;196(3):303–10.
47. He W, Ladinsky MS, Huey-Tubman KE, Jensen GJ, McIntosh JR, Björkman PJ. FcRn-mediated antibody transport across epithelial cells revealed by electron tomography. Nature. 2008;455(7212):542–46.

48. Roopenian DC, Akilesh S. FcRn: the neonatal Fc receptor comes of age. Nat Rev Immunol. 2007;7(9):715–25.
49. Ward ES, Zhou J, Ghetie V, Ober RJ. Evidence to support the cellular mechanism involved in serum IgG homeostasis in humans. Int Immunol. 2003;15(2):187–95.
50. Rhee JH, Lee SE, Kim SY. Mucosal vaccine adjuvants update. Clin Exp Vaccine Res. 2012;1(1):50–63.
51. Iwasaki A, Omer SB. Why and how vaccines work. Cell. 2020;183(2):290–95.
52. Correa VA, Portilho AI, De Gaspari E. Vaccines, adjuvants and key factors for mucosal immune response. Immunology. 2022;167(2):124–38.
53. Norton EB, Lawson LB, Freytag LC, Clements JD. Characterization of a mutant Escherichia coli heat-labile toxin, LT(R192G/L211A), as a safe and effective oral adjuvant. Clin Vaccine Immunol. 2011;18(4):546–51.
54. Lebens M, Terrinoni M, Karlsson SL, Larena M, Gustafsson-Hedberg T, Källgård S, et al. Construction and preclinical evaluation of mmCT, a novel mutant cholera toxin adjuvant that can be efficiently produced in genetically manipulated Vibrio cholerae. Vaccine. 2016;34(18):2121–8.
55. Molina Estupiñan JL, Aradottir Pind AA, Foroutan Pajoohian P, Jonsdottir I, Bjarnarson SP. The adjuvants dmLT and mmCT enhance humoral immune responses to a pneumococcal conjugate vaccine after both parenteral or mucosal immunization of neonatal mice. Front Immunol. 2023;13:1078904.
56. Ma C, Li Y, Wang L, Zhao G, Tao X, Tseng CTK, et al. Intranasal vaccination with recombinant receptor-binding domain of MERS-CoV spike protein induces much stronger local mucosal immune responses than subcutaneous immunization: implication for designing novel mucosal MERS vaccines. Vaccine. 2014;32(18):2100–08.
57. Li CJ, Jiang CL, Chao TL, Lin SY, Tsai YM, Chao CS, et al. Elicitation of potent neutralizing antibodies in obese mice by ISA 51-adjuvanted SARS-CoV-2 spike RBD-Fc vaccine. Appl Microbiol Biotechnol. 2023;107(9):2983–95.
58. Du Y, Xu Y, Feng J, Hu L, Zhang Y, Zhang B, et al. Intranasal administration of a recombinant RBD vaccine induced protective immunity against SARS-CoV-2 in mouse. Vaccine. 2021;39(16):2280–87.
59. Stanberry LR, Simon JK, Johnson C, Robinson PL, Morry J, Flack MR, et al. Safety and immunogenicity of a novel nanoemulsion mucosal adjuvant W805EC combined with approved seasonal influenza antigens. Vaccine. 2012;30(2):307–16.
60. Hsieh CL, Goldsmith JA, Schaub JM, DiVenere AM, Kuo HC, Javanmardi K, et al. Structure-based design of prefusion-stabilized SARS-CoV-2 spikes. Science. 2020;369(6510):1501–05.
61. Li T, Zheng Q, Yu H, Wu D, Xue W, Xiong H, et al. SARS-CoV-2 spike produced in insect cells elicits high neutralization titres in non-human primates. Emerg Microbes Infect. 2020;9(1):2076–90.
62. Tessier DC, Thomas DY, Khouri HE, Laliberié F, Vernet T. Enhanced secretion from insect cells of a foreign protein fused to the honeybee melittin signal peptide. Gene. 1991;98(2):177–83.
63. Soppela S, Plavec Z, Gröhn S, Mustonen I, Jartti M, Oikarinen S, et al. Immunological and structural evaluation of the intranasally administrated CVB1 whole-virus and VLP vaccines. Sci Rep. 2025;15(1):10198.
64. Jalkanen P, Pasternack A, Maljanen S, Melén K, Kolehmainen P, Huttunen M, et al. A combination of N and S antigens with IgA and IgG measurement strengthens the accuracy of SARS-CoV-2 Serodiagnostics. J Infect Dis. 2021;224(2):218–28.
65. Schindelin J, Arganda-Carreras I, Frise E, Kaynig V, Longair M, Pietzsch T, et al. Fiji: an open-source platform for biological-image analysis. Nat Methods. 2012;9(7):676–82.
66. Soppela S. Production of novel engineered enterovirus-like particles. 2021 [cited 2025 Nov 26]. Available from: https://trepo.tuni.fi/handle/10024/136060.
67. Lehto H. Screening optimal vaccine adjuvants for recombinant protein-based coronavirus vaccine. 2024 [cited 2025 Nov 26]. Available from: https://www.utupub.fi/handle/10024/178142.
68. Luckow B, Lehmann MH. A simplified method for bronchoalveolar lavage in mice by orotracheal intubation avoiding tracheotomy. BioTechniques. 2021;71(4):534–37.
69. Lampinen V, Gröhn S, Soppela S, Blazevic V, Hytönen VP, Hankaniemi MM. SpyTag/SpyCatcher display of influenza M2e peptide on norovirus-like particle provides stronger immunization than direct genetic fusion. Front Cell Infect Microbiol. 2023;13:1216364.
70. Wrapp D, Wang N, Corbett KS, Goldsmith JA, Hsieh CL, Abiona O, et al. Cryo-EM structure of the 2019-nCoV spike in the prefusion conformation. Science. 2020;367(6483):1260–63.
71. Makidon PE, Bielinska AU, Nigavekar SS, Janczak KW, Knowlton J, Scott AJ, et al. Pre-clinical evaluation of a novel nanoemulsion-based hepatitis B mucosal vaccine. PLoS One. 2008;3(8):e2954.
72. U.S. Department of Health and Human Services, Food and Drug Administration, Center for Biologics Evaluation and Research. Guidance for industry: characterization and qualification of cell substrates and other biological materials used in the production of viral vaccines for infectious disease indications. Rockville (MD): Food and Drug Administration; 2010.
73. Cervarix | European Medicines Agency (EMA). 2018 [cited 2025 Oct 3]. Available from: https://www.ema.europa.eu/en/medicines/human/EPAR/cervarix.
74. Xu H, Alzhrani RF, Warnken ZN, Thakkar SG, Zeng M, Smyth HDC, et al. Immunogenicity of antigen adjuvanted with AS04 and its deposition in the upper respiratory tract after intranasal administration. Mol Pharm. 2020;17(9):3259–69.
75. Lungwitz U, Breunig M, Blunk T, Göpferich A. Polyethylenimine-based non-viral gene delivery systems. Eur J Pharm Biopharm Off J Arbeitsgemeinschaft Pharm Verfahrenstech EV. 2005;60(2):247–66.
76. Günther M, Lipka J, Malek A, Gutsch D, Kreyling W, Aigner A. Polyethylenimines for RNAi-mediated gene targeting in vivo and siRNA delivery to the lung. Eur J Pharm Biopharm Off J Arbeitsgemeinschaft Pharm Verfahrenstech EV. 2011;77(3):438–49.
77. Sheppard NC, Brinckmann SA, Gartlan KH, Puthia M, Svanborg C, Krashias G, et al. Polyethyleneimine is a potent systemic adjuvant for glycoprotein antigens. Int Immunol. 2014;26(10):531–38.
78. Coronavirus disease (COVID-19) | WHO - Prequalification of Medical products (IVDs, medicines, vaccines and immunization devices, vector control). [cited 2025 Sept 10]. Available from: https://extranet.who.int/prequal/vaccines/coronavirus-disease-covid-19.
79. COVID-19 Market Dashboard | UNICEF Supply Division. [cited 2025 Sept 11]. Available from: https://www.unicef.org/supply/covid-19-market-dashboard.
80. Titball RW, Bernstein DI, Fanget NVJ, Hall RA, Longet S, MacAry PA, et al. Progress with COVID vaccine development and implementation. Npj Vaccines. 2024;9(1):69.
81. Mostaghimi D, Valdez CN, Larson HT, Kalinich CC, Iwasaki A. Prevention of host-to-host transmission by SARS-CoV-2 vaccines. Lancet Infect Dis. 2022;22(2):e52–8.
82. DeGrace MM, Ghedin E, Frieman MB, Krammer F, Grifoni A, Alisoltani A, et al. Defining the risk of SARS-CoV-2 variants on immune protection. Nature. 2022;605(7911):640–52.
83. Wang R, Hozumi Y, Yin C, Wei GW. Decoding SARS-CoV-2 transmission and Evolution and ramifications for COVID-19 diagnosis, vaccine, and Medicine. J Chem Inf Model. 2020;60(12):5853–65.
84. Focosi D, Maggi F, Casadevall A. Mucosal vaccines, sterilizing immunity, and the future of SARS-CoV-2 virulence. Viruses. 2022;14(2):187.
85. Walensky RP, Walke HT, Fauci AS. SARS-CoV-2 variants of concern in the United States-challenges and opportunities. JAMA. 2021;325(11):1037–38.
86. Lange J, Rivera-Ballesteros O, Buggert M. Human mucosal tissue-resident memory T cells in health and disease. Mucosal Immunol. 2022;15(3):389–97.
87. Clark RA. Resident memory T cells in human health and disease. Sci Transl Med. 2015;7(269):269rv1.
88. Grau-Expósito J, Sánchez-Gaona N, Massana N, Suppi M, Astorga-Gamaza A, Perea D, et al. Peripheral and lung resident memory T cell responses against SARS-CoV-2. Nat Commun. 2021;12:3010.
89. Nguyen TH, McAuley JL, Kim Y, Zheng MZ, Gherardin NA, Godfrey DI, et al. Influenza, but not SARS-CoV-2, infection induces a rapid interferon response that wanes with age and diminished tissue-resident memory CD8+ T cells. Clin Transl Immunol. 2021;10(1):e1242.
90. Choi SJ, Kim DU, Noh JY, Kim S, Park SH, Jeong HW, et al. T cell epitopes in SARS-CoV-2 proteins are substantially conserved in the omicron variant. Cell Mol Immunol. 2022;19(3):447–48.
91. Sette A, Crotty S. Adaptive immunity to SARS-CoV-2 and COVID-19. Cell. 2021;184(4):861–80.
92. Syed AM, Ciling A, Khalid MM, Sreekumar B, Chen PY, Kumar GR, et al. Omicron mutations enhance infectivity and reduce antibody neutralization of SARS-CoV-2 virus-like particles. medRxiv. 2022, 2021.12.20.21268048.
93. Flament H, Rouland M, Beaudoin L, Toubal A, Bertrand L, Lebourgeois S, et al. Outcome of SARS-CoV-2 infection is linked to MAIT cell activation and cytotoxicity. Nat Immunol. 2021;22(3):322–35.
94. Parrot T, Gorin JB, Ponzetta A, Maleki KT, Kammann T, Emgård J, et al. MAIT cell activation and dynamics associated with COVID-19 disease severity. Sci Immunol. 2020;5(51):eabe1670.

95. van Wilgenburg B, Scherwitzl I, Hutchinson EC, Leng T, Kurioka A, Kulicke C, et al. MAIT cells are activated during human viral infections. Nat Commun. 2016;7:11653.
96. Amini A, Klenerman P, Provine NM. Role of mucosal-associated invariant T cells in coronavirus disease 2019 vaccine immunogenicity. Curr Opin Virol. 2024;67:101412.
97. Downey AM, Kapłonek P, Seeberger PH. MAIT cells as attractive vaccine targets. FEBS Lett. 2019;593(13):1627–40.
98. Liang HY, Wu Y, Yau V, Yin HX, Lowe S, Bentley R, et al. SARS-CoV-2 variants, current vaccines and therapeutic implications for COVID-19. Vaccines. 2022;10(9):1538.
99. Zhao F, Zai X, Zhang Z, Xu J, Chen W. Challenges and developments in universal vaccine design against SARS-CoV-2 variants. Npj Vaccines. 2022;7(1):167.
100. Xu K, Gao P, Liu S, Lu S, Lei W, Zheng T, et al. Protective prototype-beta and delta-omicron chimeric RBD-dimer vaccines against SARS-CoV-2. Cell. 2022;185(13):2265–78.e14.
101. Liang Y, Zhang J, Yuan RY, Wang MY, He P, Su JG, et al. Design of a mutation-integrated trimeric RBD with broad protection against SARS-CoV-2. Cell Discov. 2022;8:17.
102. Cohen AA, Gnanapragasam PNP, Lee YE, Hoffman PR, Ou S, Kakutani LM, et al. Mosaic nanoparticles elicit cross-reactive immune responses to zoonotic coronaviruses in mice. Science. 2021;371(6530):735–41.
103. Walls AC, Miranda MC, Schäfer A, Pham MN, Greaney A, Arunachalam PS, et al. Elicitation of broadly protective sarbecovirus immunity by receptor-binding domain nanoparticle vaccines. Cell. 2021;184(21):5432–47.e16.
104. Slifka MK, Amanna IJ. Role of multivalency and antigenic threshold in generating protective antibody responses. Front Immunol. 2019;10:956.
105. Du L, Zhao G, He Y, Guo Y, Zheng BJ, Jiang S, et al. Receptor-binding domain of SARS-CoV spike protein induces long-term protective immunity in an animal model. Vaccine. 2007;25(15):2832–38.
106. Li Y, Du L, Qiu H, Zhao G, Wang L, Zhou Y, et al. A recombinant protein containing highly conserved hemagglutinin residues 81–122 of influenza H5N1 induces strong humoral and mucosal immune responses. Biosci Trends. 2013 [cited 2025 Sept 10]. Available from: http://www.biosciencetrends.com/getabstract.php?id=679.
107. Kudriavtsev AV, Vakhrusheva AV, Kryuchkov NA, Frolova ME, Blagodatskikh KA, Ivanishin TV, et al. Safety and immunogenicity of betuvax-CoV-2, an RBD-Fc-based SARS-CoV-2 recombinant vaccine: preliminary results of the first-in-human, randomized, double-blind, placebo-controlled phase I/II clinical trial. Vaccines. 2023;11(2):326.
108. Sun S, He L, Zhao Z, Gu H, Fang X, Wang T, et al. Recombinant vaccine containing an RBD-Fc fusion induced protection against SARS-CoV-2 in nonhuman primates and mice. Cell Mol Immunol. 2021;18(4):1070–73.
109. Sun Y, Li Q, Luo Y, Zhu H, Xu F, Lu H, et al. Development of an RBD-Fc fusion vaccine for COVID-19. Vaccine X. 2024;16:100444.
110. Zhang Y, Wu Y, Zhang MQ, Rao H, Zhang Z, He X, et al. An RBD-Fc mucosal vaccine provides variant-proof protection against SARS-CoV-2 in mice and hamsters. Npj Vaccines. 2025;10(1):100.
111. Laotee S, Duangkaew M, Jivapetthai A, Tharakhet K, Kaewpang P, Prompetchara E, et al. CHO-produced RBD-Fc subunit vaccines with alternative adjuvants generate immune responses against SARS-CoV-2. PLoS One. 2023;18(7):e0288486.
112. Sanda M, Morrison L, Goldman R. N- and O-glycosylation of the SARS-CoV-2 spike protein. Anal Chem. 2021;93(4):2003–09.
113. Casalino L, Gaieb Z, Goldsmith JA, Hjorth CK, Dommer AC, Harbison AM, et al. Beyond shielding: the roles of Glycans in the SARS-CoV-2 spike protein. ACS Cent Sci. 2020;6(10):1722–34.
114. Zhao X, Chen H, Wang H. Glycans of SARS-CoV-2 spike protein in virus infection and antibody production. Front Mol Biosci. 2021;8. https://www.frontiersin.org/journals/molecular-biosciences/articles/10.3389/fmolb.2021.629873/full.
115. Grant OC, Montgomery D, Ito K, Woods RJ. Analysis of the SARS-CoV-2 spike protein glycan shield reveals implications for immune recognition. Sci Rep. 2020;10(1):14991.
116. Correia R, Fernandes B, Alves PM, Carrondo MJT, Roldão A. Improving influenza HA-Vlps production in insect high five cells via adaptive laboratory evolution. Vaccines. 2020;8(4):589.
117. Yamaji H, Konishi E. Production of Japanese encephalitis virus-like particles in insect cells. Bioengineered. 2013;4(6):438–42.
118. Dai S, Zhang T, Zhang Y, Wang H, Deng F. Zika virus baculovirus-expressed virus-like particles induce neutralizing antibodies in mice. Virol Sin. 2018;33(3):213–26.
119. Renner TM, Stuible M, Rossotti MA, Rohani N, Cepero-Donates Y, Sauvageau J, et al. Modifying the glycosylation profile of SARS-CoV-2 spike-based subunit vaccines alters focusing of the humoral immune response in a mouse model. Commun Med. 2025;5(1):111.
120. Jia Q, Bielefeldt-Ohmann H, Maison RM, Masleša-Galić S, Cooper SK, Bowen RA, et al. Replicating bacterium-vectored vaccine expressing SARS-CoV-2 membrane and nucleocapsid proteins protects against severe COVID-19-like disease in hamsters. Npj Vaccines. 2021;6(1):47.
121. Thura M, En Sng JX, Ang KH, Li J, Gupta A, Hong JM, et al. Targeting intra-viral conserved nucleocapsid (N) proteins as novel vaccines against SARS-CoVs. Biosci Rep. 2021;41(9).
122. Matchett WE, Joag V, Stolley JM, Shepherd FK, Quarnstrom CF, Mickelson CK, et al. Cutting edge: nucleocapsid vaccine elicits spike-independent SARS-CoV-2 protective immunity. J Immunol. 2021;207(2):376–79.
123. Primard C, Monchâtre-Leroy E, Del Campo J, Valsesia S, Nikly E, Chevandier M, et al. OVX033, a nucleocapsid-based vaccine candidate, provides broad-spectrum protection against SARS-CoV-2 variants in a hamster challenge model. Front Immunol. 2023;14:1188605.
124. Arieta CM, Xie YJ, Rothenberg DA, Diao H, Harjanto D, Meda S, et al. The T-cell-directed vaccine BNT162b4 encoding conserved non-spike antigens protects animals from severe SARS-CoV-2 infection. Cell. 2023;186(11):2392–409.e21.
125. Coléon S, Wiedemann A, Surénaud M, Lacabaratz C, Hue S, Prague M, et al. Design, immunogenicity, and efficacy of a pan-sarbecovirus dendritic-cell targeting vaccine. eBiomedicine. 2022;80:104062.
126. Rabdano SO, Ruzanova EA, Vertyachikh AE, Teplykh VA, Emelyanova AB, Rudakov GO, et al. N-protein vaccine is effective against COVID-19: phase 3, randomized, double-blind, placebo-controlled clinical trial. J Infect. 2024;89(5):106288.
127. Chiuppesi F, Nguyen VH, Park Y, Contreras H, Karpinski V, Faircloth K, et al. Synthetic multiantigen MVA vaccine COH04S1 protects against SARS-CoV-2 in Syrian hamsters and non-human primates. Npj Vaccines. 2022;7(1):7.
128. Rice A, Verma M, Shin A, Zakin L, Sieling P, Tanaka S, et al. Intranasal plus subcutaneous prime vaccination with a dual antigen COVID-19 vaccine elicits T-cell and antibody responses in mice. Sci Rep. 2021;11(1):14917.
129. Huang Y, Chen J, Chen S, Huang C, Li B, Li J, et al. Molecular characterization of SARS-CoV-2 nucleocapsid protein. Front Cell Infect Microbiol. 2024;14. https://www.frontiersin.org/journals/cellular-and-infection-microbiology/articles/10.3389/fcimb.2024.1415885/full.
130. Moss P. The T cell immune response against SARS-CoV-2. Nat Immunol. 2022;23(2):186–93.
131. Grifoni A, Weiskopf D, Ramirez SI, Mateus J, Dan JM, Moderbacher CR, et al. Targets of T cell responses to SARS-CoV-2 coronavirus in humans with COVID-19 disease and unexposed individuals. Cell. 2020;181(7):1489–501.e15.
132. Zhang XY, Guo J, Wan X, Zhou JG, Jin WP, Lu J, et al. Biochemical and antigenic characterization of the structural proteins and their post-translational modifications in purified SARS-CoV-2 virions of an inactivated vaccine candidate. Emerg Microbes Infect. 2020;9(1):2653–62.
133. Yu S, Wei Y, Liang H, Ji W, Chang Z, Xie S, et al. Comparison of physical and biochemical characterizations of SARS-CoV-2 inactivated by different treatments. Viruses. 2022;14(9):1938.
134. Lopez-Munoz AD, Kosik I, Holly J, Yewdell JW. Cell surface SARS-CoV-2 nucleocapsid protein modulates innate and adaptive immunity. Sci Adv. 2022;8(31).
135. Fielding CA, Sabberwal P, Williamson JC, Greenwood EJD, Crozier TWM, Zelek W, et al. SARS-CoV-2 host-shutoff impacts innate NK cell functions, but antibody-dependent NK activity is strongly activated through non-spike antibodies. eLife. 2022;11.
136. Peng Y, Felce SL, Dong D, Penkava F, Mentzer AJ, Yao X, et al. An immunodominant NP105-113-B*07: 02 cytotoxic T cell response controls viral replication and is associated with less severe COVID-19 disease. Nat Immunol. 2022;23(1):50–61.
137. Peng H, Tao YL, Yun WL, Li J, Huang J, Qiang LZ, et al. Long-lived memory T lymphocyte responses against SARS coronavirus nucleocapsid protein in SARS-recovered patients. Virology. 2006;351(2):466–75.
138. Tso FY, Lidenge SJ, Poppe LK, Peña PB, Privatt SR, Bennett SJ, et al. Presence of antibody-dependent cellular cytotoxicity (ADCC) against SARS-CoV-2 in COVID-19 plasma. PLoS One. 2021;16(3):e0247640.
139. Hagemann K, Riecken K, Jung JM, Hildebrandt H, Menzel S, Bunders MJ, et al. Natural killer cell-mediated ADCC in SARS-CoV-2-infected individuals and vaccine recipients. Eur J Immunol. 2022;52(8):1297–307.

140. Yu Y, Wang M, Zhang X, Li S, Lu Q, Zeng H, et al. Antibody-dependent cellular cytotoxicity response to SARS-CoV-2 in COVID-19 patients. Signal Transduct Target Ther. 2021;6(1).
141. Le Bert N, Tan AT, Kunasegaran K, Tham CYL, Hafezi M, Chia A, et al. SARS-CoV-2-specific T cell immunity in cases of COVID-19 and SARS, and uninfected controls. Nature. 2020;584(7821):457–62.
142. Renegar KB, Small PA, Boykins LG, Wright PF. Role of IgA versus IgG in the control of influenza viral infection in the murine respiratory tract. J Immunol. 2004;173(3):1978–86.
143. Lapuente D, Fuchs J, Willar J, Vieira Antão A, Eberlein V, Uhlig N, et al. Protective mucosal immunity against SARS-CoV-2 after heterologous systemic prime-mucosal boost immunization. Nat Commun. 2021;12(1):6871.
144. Kwonll D-i, Mao T, Israelow B, Santos Guedes de Sá K, Dong H, Iwasaki A. Mucosal unadjuvanted booster vaccines elicit local IgA responses by conversion of pre-existing immunity in mice. Nat Immunol. 2025;26(6):908–19.

Publisher's Note